UNIVERSITY OF INDONESIA

SEISMIC SIMULTANEOUS INVERSION METHOD FOR RESERVOIR HYDROCARBON CHARACTERIZATION: A STUDY AT UG MASSIVE FORMATION OF JAVAZ FIELD, WEST NATUNA BASIN INDONESIA

THESIS

YUVID DWI R
1 0 0 6 7 3 3 8 7 1

UNIVERSITY OF INDONESIA
FACULTY OF MATHEMATICS AND NATURAL SCIENCES
PHYSICS GRADUATE PROGRAM
RESERVOIR GEOPHYSICS SECTION
JAKARTA
JUNE – 2012

UNIVERSITY OF INDONESIA

SEISMIC SIMULTANEOUS INVERSION METHOD FOR RESERVOIR HYDROCARBON CHARACTERIZATION: A STUDY AT UG MASSIVE FORMATION OF JAVAZ FIELD, WEST NATUNA BASIN INDONESIA

THESIS
Proposed for partially fulfill one of the requirements to earn degree Master of Science

YUVID DWI R
1 0 0 6 7 3 3 8 7 1

UNIVERSITY OF INDONESIA
FACULTY OF MATHEMATICS AND NATURAL SCIENCES
PHYSICS GRADUATE PROGRAM
RESERVOIR GEOPHYSICS SECTION
JAKARTA
JUNE – 2012

STATEMENT OF ORIGINALITY

This thesis is my own work, and all good sources quoted or

referred to I have stated correctly

Name   : Yuvid Dwi R

SID   : 1006733871

Sign   :

Date   : 8 June 2012

APPROVAL SHEET

Thesis submitted by

Name	:	Yuvid Dwi R
NPM	:	1006733871
Study program	:	Reservoir Geophysics
Thesis title	:	Seismic Simultaneous Inversion Method for Hydrocarbon Reservoir Characterization: A Study at UG Massive Formation of Javaz Field, West Natuna Basin, Indonesia

Has been approved by committee member and accepted in partial fulfillment of the requirement for the Degree of Master of Science in Reservoir Geophysics, Faculty of Mathematics and Natural Sciences, University of Indonesia.

BOARD OF EXAMINERS

Supervisor : Dr. rer. nat. Abdul Haris (..)

Examiner : Prof. Dr. Suprajitno Munadi (..)

Examiner : Dr. Ricky Adi Wibowo (..)

Examiner : Dr. Charlie Wu (..)

Defense date: June 8th, 2012

ACKNOWLEDGMENT

Alhamdulillah, thank you to Allah SWT, Who has provided the opportunity for authors, given His affection and facilitate the process until this thesis can be completed on time. Writing of this thesis is a prerequisite for achieving a degree of Master of Science Reservoir Geophysics, University of Indonesia. I realize that the writing of this thesis is not easy, without the help and guidance of the various parties it may be very difficult to realize. Therefore, my sincere gratitude to:

(1) Dr. rer. nat Abdul Haris as supervisor who have helped with the sincere and willing to provide input and guidance in completing this thesis.

(2) Prof.Dr. Suprayitno Munadi, Dr. Ricky Adi Wibowo dan Dr. Charlie Wu who has given a lot of input, suggestions and advice, and willingness to examiner and do not forget to thank to the entire administrative staff of University of Indonesia that has a lot of help during this learning process

(3) Beloved mother who always prayed every time, my wife and beloved sons and daughters who patiently, praying and giving encouragement so that this thesis can be completed.

(4) Management of ConocoPhillips Indonesia who have given support and permission to use the data in this thesis, as well as my friends at work and college.

Finally, the author of this thesis realizes that there are still many shortcomings in this thesis however; the authors hope that this thesis can provide benefits for those who need it. Who is serious then he will succeed "Man Jadda WaJada"

Jakarta, June 2012

Author

APPROVAL FOR PUBLICATION SCIENTIFIC
FOR ACADEMIC PURPOSE

As an academic community of University of Indonesia, I am the undersigned

Name	: Yuvid Dwi R
NPM	: 1006733871
Study Program	: Physics Graduate Program
Specificity	: Reservoir Geophysics Section
The kind of work	: Thesis

With the spirit of supporting knowledge sharing, herewith I would like to legalize University of Indonesia to have the non-exclusive royalty free rights for my thesis paper titled:

"Seismic Simultaneous Inversion Method for Reservoir Hydrocarbon Characterization: A Study at UG Massive Formation of Javaz Field, West Natuna Basin, Indonesia"

With this right, University of Indonesia would be able to store, reformat, manage, maintain, and also publish my thesis paper as long as they still stated my name as the writer or owner of this copy rights. I make this statement with the truth

Created at: Jakarta

Date: June 2012

Stated by,

(Yuvid Dwi R)

ABSTRACT

Name   : Yuvid Dwi R

Study Program   : Reservoir Geophysics Graduate Program

Title   : Seismic Simultaneous Inversion Method for Reservoir Hydrocarbon Characterization: A Study at UG Massive Formation of Javaz Field, West Natuna Basin, Indonesia

UG Massive formation is the main reservoir of Javaz field, oil and gas producing field, situated in West Natuna Basin. The use of acoustic impedance (P-Impedance) only to characterize reservoir hydrocarbon in this field will lead us into large uncertainty. Therefore, to overcome that issue, Seismic Simultaneous Inversion method is used at Javaz field within UG Massive formation interval. This method is applied as an alternative method to predict the pore gas (*Lambda-Rho*) and porosity distribution, using partial post stack 3D seismic data which are inverted simultaneously; then Javaz-4 well data which will be used as a reference well for predicting reservoir properties in other wells at Javaz field.

Seismic Simultaneous Inversion method resulted Javaz-3 well has similar reservoir properties as studied in Javaz-4 well. However, Javaz-1A and Javaz-2 showed different result caused by large uncertainty in seismic resolution (poor quality seismic data). Porosity and pore gas prediction suggested around 20 to 30 percent and 13 to 18 GPa*g/cc respectively, throughout the field. Hence, this method could be used as an alternative to predict UG Massive reservoir properties in Javaz field away from the wells, and it could be applied to the same field with large uncertainty.

Key words:

Porosity, Pore gas (*Lambda-Rho*), *Seismic simultaneous inversion*

University of Indonesia

ABSTRAK

Nama   : Yuvid Dwi R
Program Study   : Reservoir Geophysics Graduate Program
Judul   : Seismic Simultaneous Inversion Method for Reservoir
                              Hydrocarbon Characterization: A Study at UG Massive
                              Formation of Javaz Field, West Natuna Basin, Indonesia

Formasi UG Massive merupakan reservoar utama pada lapangan Javaz, lapangan ini memproduksi minyak dan gas dan berada pada cekungan Natuna Barat. *Study* yang dilakukan untuk mengkarakterisasi *reservoir hydrocarbon* pada lapangan ini jika hanya menggunakan akustik impedance (P-Impedance) saja akan menimbulkan ketidakpastian, untuk mengatasi hal ini maka metode *Seismic simultaneous inversion* digunakan pada lapangan Javaz dengan target formasi UG Massive. Metode ini digunakan sebagai alternative untuk memprediksi sebaran pore gas (*Lambd-Rho*) dan porositas, dengan menggunakan partial post stack 3D seismic data yang di inversikan secara bersamaan dan satu sumur (Javaz-4) data yang digunakan sebagai kontrol untuk kemudian dijadikan acuan dalam memprediksi karakter reservoir para area sumur lainnya.

Dengan menggunakan metode *Seismic simultaneous inversion* ini, maka didapatkan hasil prediksi karakter reservoir pada sumur Javaz-3 yang memiliki karakter mendekati sumur Javaz-4 pada formasi utama, namun tidak demikian untuk sumur Javaz-2 dan Javaz-1A. Untuk perkiraan sebaran porositas maupun pore gas didapatkan hasil yang cukup baik, dengan nilai porositas berkisar antara 20% hingga 30% dan pore gas (*Lambda-Rho*) yang berkisar antara 13 (GPa*g/cc) hingga 18 (GPa*g/cc). Dari hasil *study* ini maka dapat disimpulkan bahwa metode ini dapat digunakan sebagai alternative untuk memprediksi karakter reservoar pada formasi UG Massive.

Kata kunci:
Porositas, Pore gas (*Lambda-Rho*), *Seismic simultaneous inversion*

University of Indonesia

TABLE OF CONTENTS

Table of Figures

University of Indonesia

Table of Tables

CHAPTER 1
INTRODUCTION

1.1 Background

Since the 20th century, the oil and gas industry has been the largest the primary industry for providing energy and supporting modern human life. Although alternative energy sources such as geothermal, coal, nuclear, and others are being developed and produced, oil and gas are still the major sources of energy. Discovering new large sources of oil and gas efficiently and effectively has become more challenging since exploration areas are limited and more complex. For decades, seismic reflection methods have been widely used in oil and gas industry to image potential reservoirs of oil and gas and provide analysis of the hydrocarbon types within the reservoir and properties of the reservoir rocks themselves.

An understanding of the regional geologic framework of a field is also required as well as detailed knowledge and comprehension of the physical properties of rocks that developed in the prospect area. With high quality seismic data, changes in rock properties such as porosity, density, fluid saturation, and others can be estimated because each has an effect on seismic signature. Changes in physical rock properties will be represented as changes of seismic acoustic impedance. The seismic inversion method, in which we can correlate changes in rock properties and fluid types to changes in acoustic impedance, can be used both qualitatively and quantitatively to predict the rock properties and fluids content within a reservoir.

Traditionally reservoir characterization only used information from P-impedance (compressional) seismic data; which has limitations in distinguishing between the effects of lithology and fluid content. S-impedance (shear) seismic data can be used to help distinguish between lithology and fluid content. Generating impedance inversions of seismic P and S separately will give inaccurate results.

Elastic impedance inversion that utilizes both P and S- impedance data will provide better results. The Seismic Simultaneous Inversion method will use partial

angle stack data (near, mid, and far angle stacks). Each partial angle stack is inverted simultaneously using wavelets extracted from each angle stack to estimate P and S-impedance (Zp and Zs). Density (ρ) estimates can also be derived from this inversion. These results have proven very useful in prediction of certain lithologies and fluid saturations. The three inversions results can be transformed into Lambda-rho ($\lambda\rho$) (*Incompressibility*) that is used to predict pore fluid content, in this case hydrocarbon potential and Mu-rho ($\mu\rho$) (*Rigidity*) that can be used to predict lithology. This parameter is sensitive to rocks matrix character. A Vp/Vs (P-velocity/S-velocity) volume is also generated to predict the density effect and help distinguish the density effects from fluid effects.

1.2 Objectives

The objectives of this study are (1) To determine the physical properties of reservoir, (2) to analyze gas and porosity distribution using well Javaz-4 at UG Massive formation in Javaz field, West Natuna Basin - Indonesia, (3) to do blind test at well Javaz-3, Javaz-2 and Javaz-1A to see if there is still good correlation from Javaz-4, (4) to prove that the Simultaneous inversion method can be used in this study and also can be used as a reference for further development in this area.

1.3 Method

The scope of this study is limited within the availability of data, area of interest and the result study. The data that will be used in this thesis are four wells and four seismic data volumes. This study is also focused in between interval 1000 to 1500 millisecond of area of interest, which is identified as the prospect. The workflow of this process (Figure 1.1) will be used to combine partial angle stack data simultaneously with low frequency models and is convoluted by a wavelet which is extracted from every angle stack to generate P-impedance (Zp), S-impedance (Zs) and density (ρ) volumes. These volumes can be used to derive Lambda-rho, Mu-rho

University of Indonesia

and Vp/Vs volumes. The volumes and results of the analysis will be used to analyze porosity distribution and gas content through horizon slice with geological control.
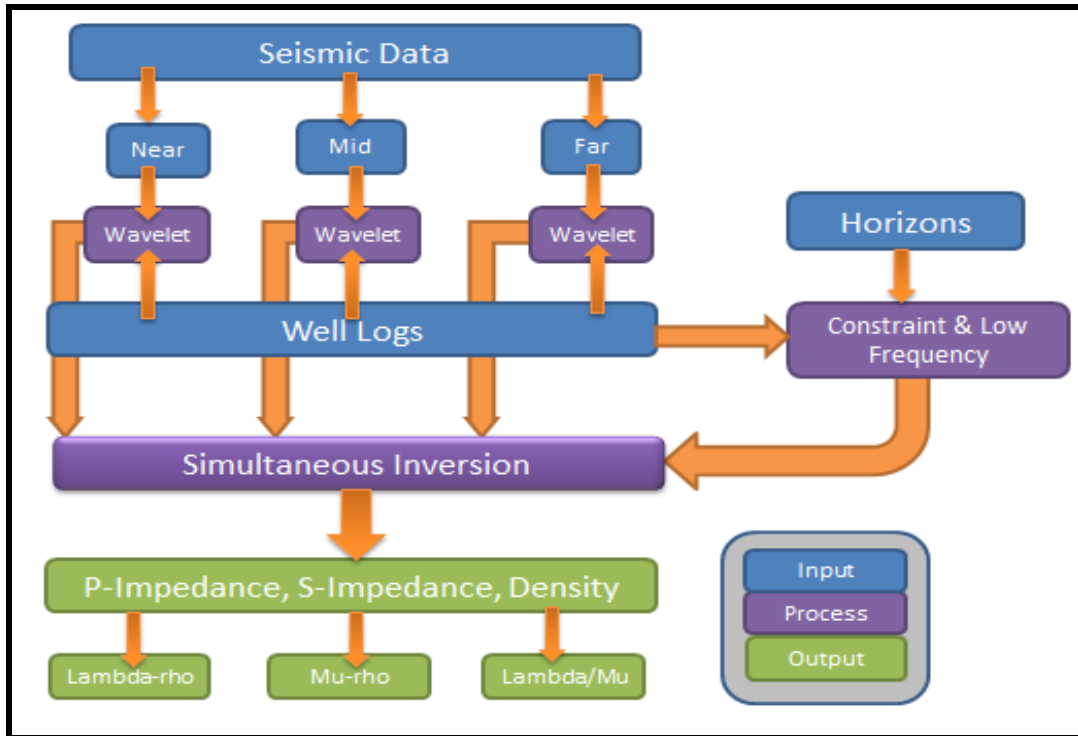
Figure 1.1 Work flow for Simultaneous Inversion (Fugro-Jason, 1993)

1.4 Object and Area of Study

The zone of interest of this study is at UG Massive formation, Javaz field at West Natuna Basin, located in the southwestern part of the South China Sea. The area is approximately 1100 km north of Jakarta, 320 km northeast of Singapore, and west of the Natuna islands between Indonesia and Malaysia on the Sunda shelf. Water depths in the area of interest are shallow (200 – 500m).

Figure 1.2 Study area of Javaz field at West Natuna Basin
(http://geoseismicseasia.blogspot.com/2008/11/luconia-basin.html)

1.5 Data Availability

The study uses data from the Javaz field data set. The data set contains 4 wells and 4 seismic volumes (Full, near, mid and far angle stack data). Only 1 of 4 well data is used for this study since only Javaz-4 well data has better seismic data compare to others. 3D seismic data is constrained within Inline 6100 – 8000 and X-line 4100 – 4700. All the wells are located within the seismic data area. The partial angle stack of seismic data are Near Stack ($5^o - 15^o$), Mid Stack ($15^o - 25^o$) and Far Stack ($25^o - 35^o$). All well logs and 3D seismic data have been properly pre-conditioned prior to use. The pre-conditioning process included environment corrections, calculations and/or conditioning processes.

Table 1.1 Well data used for study on Javaz field

GENERAL LOGS	JAVAZ-1A	JAVAZ-2	JAVAZ-3	JAVA-4
CALIPER	ok	ok	ok	ok
MULTIPLE RESISTIVITY	ok	ok	ok	ok
SP	ok	ok	ok	ok
GAMMA	ok	ok	ok	ok
SONIC-VP	ok	ok	ok	ok
SONIC-VS	-	ok	ok	ok
NPHI	ok	ok	ok	ok
RHOB	ok	ok	ok	ok
PEF	-	ok	ok	ok
ROP	ok	ok	ok	ok
MUD LOG	ok	ok	ok	ok

	Start	# of Bytes	Value
Inline Byte location:	189	4	6000
Xline Byte location:	193	4	4100
Source X Byte location:	181	4	645632
Source Y Byte location:	185	4	474746
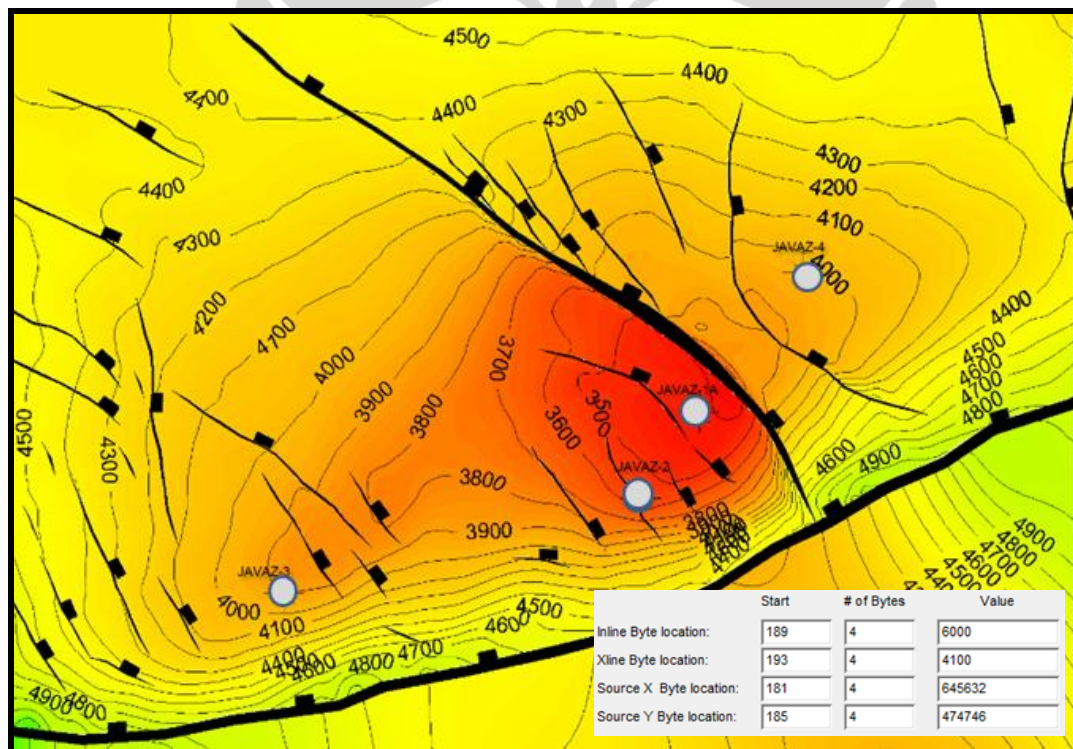
Figure 1.3 Survey area for this study containing 4 wells, which covers inline 6100 – 8000 and x-line 4100 - 4700

1.6 Writing Scheme

The structure of this thesis was designed to follow the chronological development of the project. Chapter one presents an introduction to review the background of this study, problems, aims and objectives, and scope of this thesis. Chapter two discusses review of Regional Geology and Petroleum System, which discuss the structural environment and stratigraphy and the workings of the local petroleum system. Chapter three discusses the background theories applied in the study such as seismic reflection theory, Rock physics, AVO, seismic inversion and seismic simultaneous inversion method. Chapter four discusses data processing issues such as data preparation, well seismic ties and seismic inversion processes. Chapter five concerns the analysis and interpretations of the result from this study, where prediction of porosity and pore gas are analyzed. Chapter six contains conclusions and recommendations.

CHAPTER 2
REGIONAL GEOLOGY AND PETROLEUM SYSTEM

2.1 Geology of Javaz

The Javaz field is located in the Block B, South Natuna Sea, approximately 25 km north-east of Brown field. The Javaz field is situated in the West Natuna basin. The basin formed during the Oligocene within an extensional faulting phase. This phase is related to the rifting in South Natuna Sea area. Predominantly granitic basement provided the provenance for coarse continental clastics, which filled in the basin. The UG Massive sediment was deposited in fluvial and lacustrine environments during this period.

From Late Oligocene to Middle Miocene, a compressive and wrenching phase caused structural inversion of the basin. It resulted in northwest-southeast trending right lateral movements in the Malay-Natuna Basin. Many original half-grabens were inverted into faulted anticlines (now major exploration targets). Deposition continued in a marginal marine/estuarine setting with fluvial and marginal marine deposits of the Gede, Slamet and Semeru formations. Inversion ceased by the end of Middle Miocene and a regional unconformity developed. Subsequently a regional sag phase dominated the structural regime. The resulting Rinjani shales are generally considered to be open shelf, shallow marine deposits.

The Slamet shale is extensively deposited over the entire area, and provides a regional seal for underlying reservoirs in almost the entire Block B area. The hydrocarbon charge is modeled to come from the deep rift graben beneath Javaz field. A potential migration path is mapped through the fault at depth. The lacustrine / mixed kerogen source rock is anticipated to be the source rock type charging the structure.

2.2 Structural Geology

The West Natuna basin Figure 2.1 was mainly composed by 2 main tectonic regimes, an extensional regime, which produced the Eocene – Oligocene graben phase and a compressional regime, which produced Miocene sinistral and dextral wrench faults. Two major tectonic events responsible for this compressional history are:

- The collision of Indian and Eurasian plates during the Middle Eocene (Tapponier and others, 1982)
- The collision of the Australian continental shelf with the Philippine Sea plate during the Early Miocene (Hall, 1996)

Present day, the West Natuna Basin is an inverted intracratonic rift basin within the Sundaland microplate, and is surrounded by the Philippine Sea plate to the east, the Eurasian plate to the North, and Indo-Australian plate to the South and West.
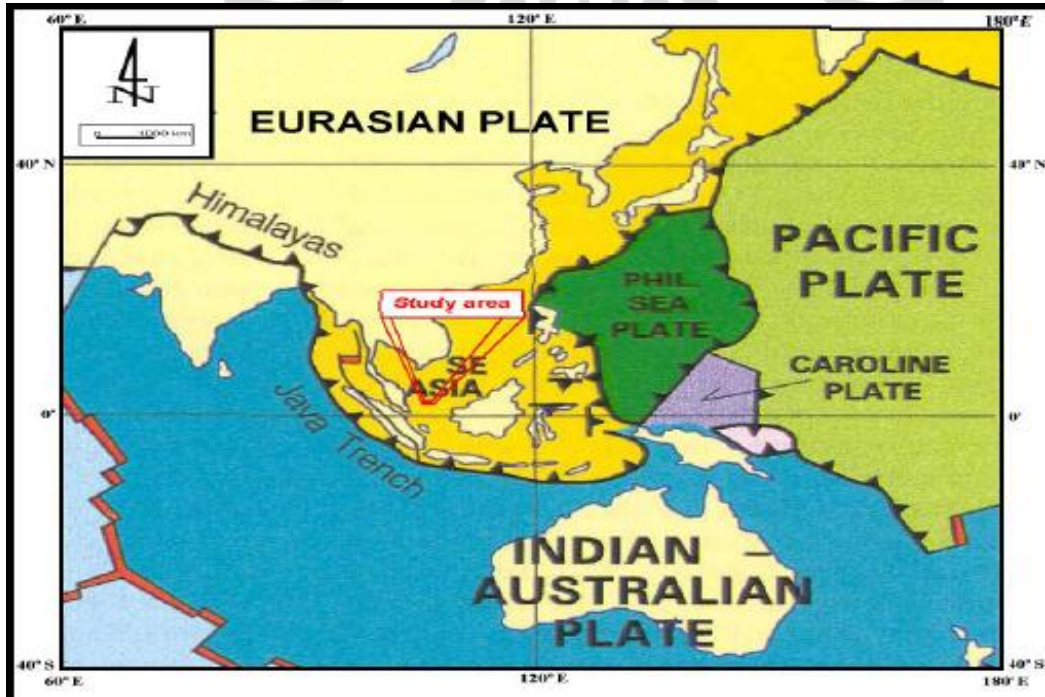
Figure 2.1 Present plate tectonic overview of study area (Daines et al, 1985).

The Javaz Field is an inverted NE-SW four-way dip structure limited by a major reverse fault to the south. This fault is cut by a series of smaller faults trending SE-NW and NE-SW. A major fault trending SE-NW with a maximum displacement of approximately 500 ft separates the western and eastern Javaz field. This fault is assumed to seal hydrocarbons in separated blocks. The Javaz reservoirs may be in communication in the water leg at the end of the fault. Communication between two blocks may also be present in juxtaposed sand between UG Massive sand in the east block and Zone-3 in west, or juxtaposed sand between Lower UG in west block and Zone-3 in east, but fault seal modeling suggests those reservoirs may be sealed along the fault plane by shale gouge. The top structure of Javaz reservoir is approximately (-3250 ft TVDSS) depth. The maximum closure area in Javaz field is approximately 3,000 acres. Figure 2.2 shows the structure map at the top of the UG Massive reservoirs in Javaz field and the fluid contacts for the UG Massive reservoirs.
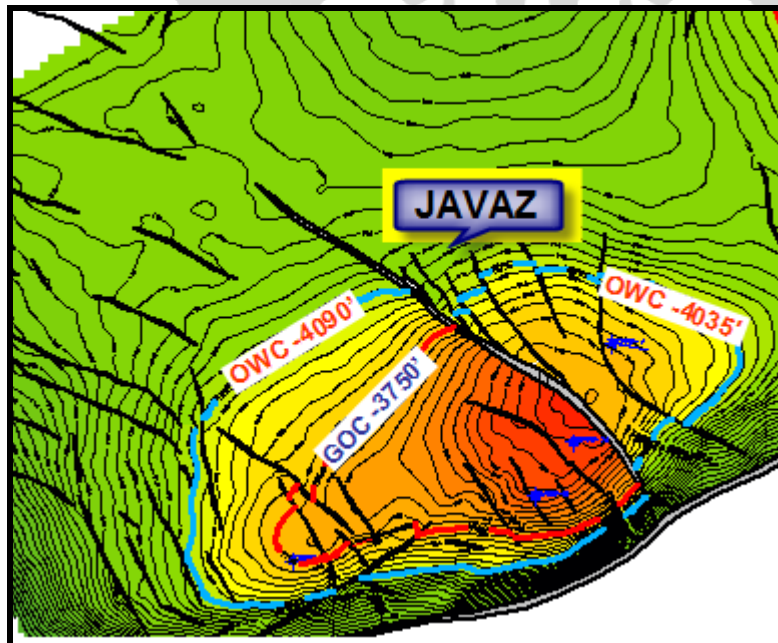
Figure 2.2 Depth structure map at top horizon Top_Javaz
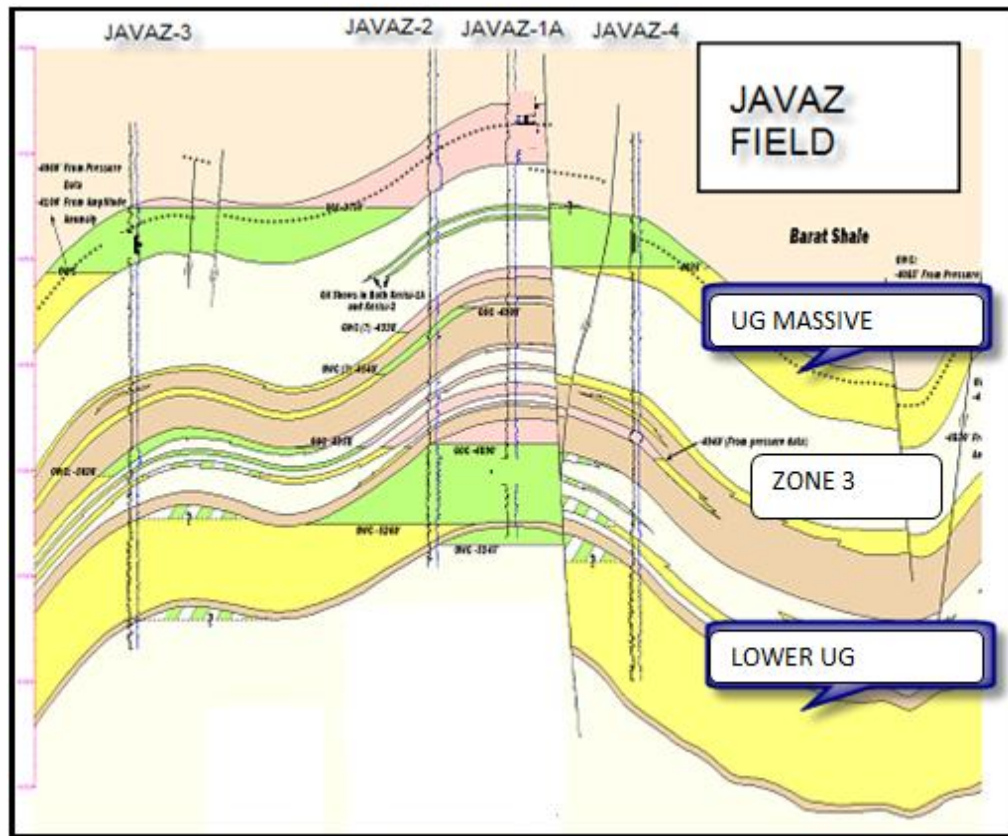
Figure 2.3 Cross section through Javaz showing the reservoir and well data (Conocophillips, 2008)

2.3 Stratigraphy

The syn-rift continental clastics of the Kerinci formation were the first sediments deposited in the Javaz area during formation of the West Natuna basin, initiated in the Eocene-Oligocene by a phase of extensional faulting. Highly variable granitic and meta-sedimentary basement provided the provenance for the formation. In several of the early syn-rift grabens, lacustrine sediments accumulated and provide a regionally important oil-prone source.

As the rifting ceased in Mid-Oligocene times, the UG Massive post-rift sag-phase sediments, the main objective in Javaz, were the first to transgress the old graben margins. These comprise regionally extensive fluvio-deltaic reservoirs. In the latest Oligocene, a compressive wrench phase caused by northwest-southeast

trending, right-lateral movement in the Malay-Natuna region, caused inversion of many of the earlier syn-rift grabens and platform areas. It caused the formation of the Javaz anticlines. The regional top seal, the Slamet brackish-lacustrine shales, were deposited in the Javaz area as a syn-inversion depocentre. However, the coeval clastics of the Gede formation were not deposited in the Javaz area, although these become important reservoirs in several other fields in the Block B area. A regional unconformity developed as the compression ceased towards the end of Middle Miocene. The deposits of the subsequent regional sag phase comprise the shallow marine deposits of the Rinjani Formation. The stratigraphy of Javaz area is shown in Figure 2.4

The main objective of the Javaz field is the UG Massive formation in the post rift section. This section was deposited as the extensional tectonic regime ceased. This makes the overall thickness of the interval relatively constant. However, the depositional direction in Javaz field was variable. The most prominent aspect that influenced the deposition of the formation is the relative Slamet lake level changes. The Slamet Lake was north of the Javaz field. The Lower UG interval was deposited as the Slamet lake level transgressed landward to the SW direction, and created a NE-SW lake embayment. This embayment had positioned Javaz field in relatively the same delta front – shoreline environment.

As the Zone-3 interval was deposited, the lake level regressed and placed Javaz field in relatively proximal-distal relationship, as the depositional direction moved towards the Slamet Lake in the NE. The log motifs in both Javaz field show a combination of isolated fining upward and coarsening upward sequences which are interpreted as distributary channels and mouthbars.
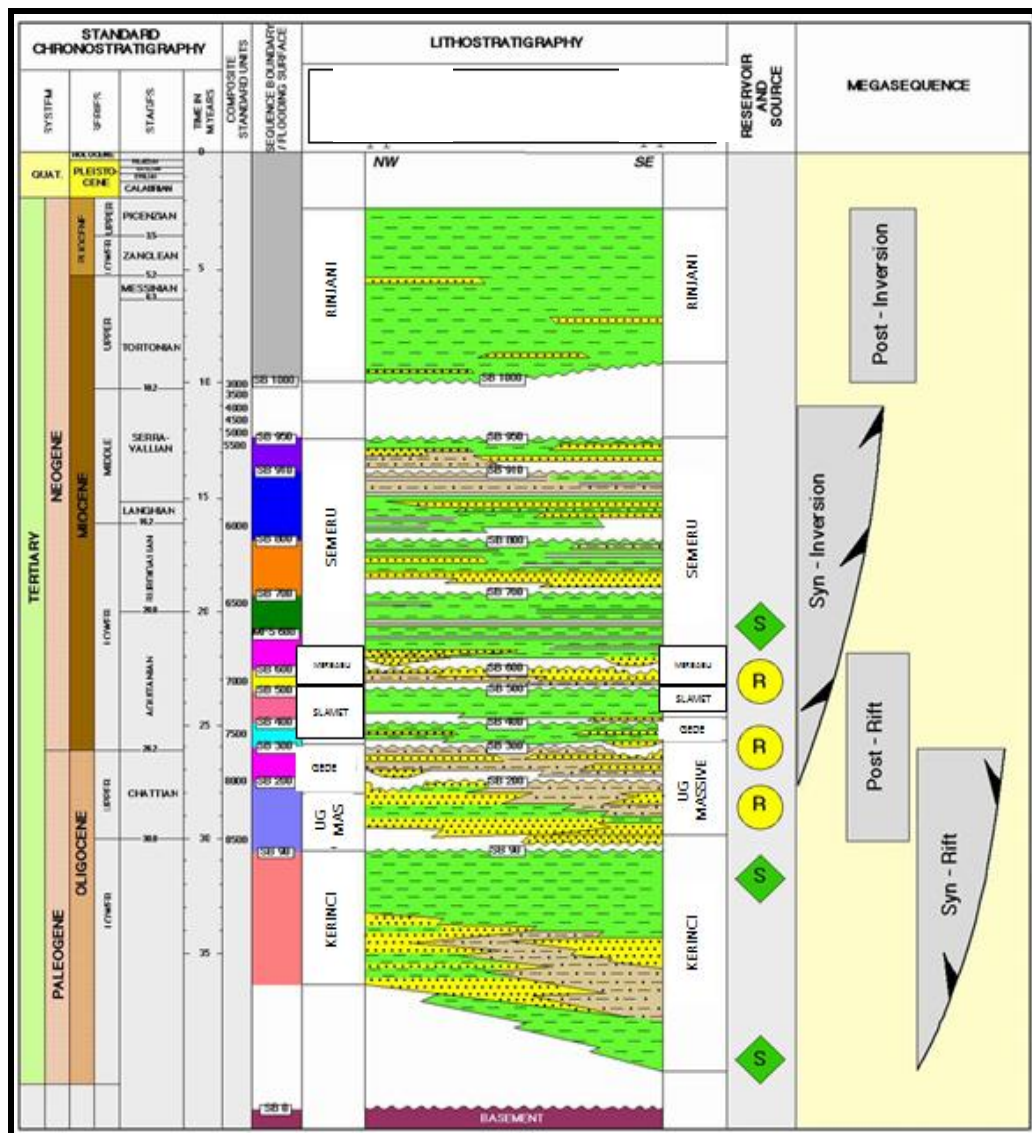
Figure 2.4 Stratigraphic column. UG formation is the main reservoir of Javaz (Conocophillips, 2008)

In the UG Massive interval, the lake level was regressed further basin ward and it placed all Javaz in fluvial environment. Relatively low sinuosity channel systems can be observed in Javaz field. Evidence for a period of confinement and amalgamation of reservoir in this system is represented by the UG Massive reservoir. The UG Massive is interpreted to be a series of amalgamated channel deposits with relatively minor overbank preservation whose deposition was localized by an underlying confining surface.

2.4 Petroleum System

2.4.1 Source Rock

During the Lower Oligocene period Kerinci formation there are two distinct source rock intervals. Generally the source rocks were deposited in a lacustrine environment. The early syn-rift open lacustrine source rock is characterized by oil-prone, algal organic matter, and late syn-rift shallow lacustrine/shoreline source rock is characterized by mixed algal and terrestrial organic matter.

2.4.2 Migration

Primary migration is the first phase of the migration process. It involves expulsion of hydrocarbons from their fine-grained, low permeability source rock into a carrier bed having much greater permeability. Secondary migration is the movement of oil and gas within this carrier bed. Migration to Jaraz initiated in the Miocene and extended into the Pleistocene. Berendson in 1991 revealed that oil had started to migrate from Kerinci formation since Late Miocene with a relative vertical trend.

2.4.3 Reservoir Rock

In Javaz field, the UG Massive formation is a good quality reservoir. The formation was deposited as fluvial to lacustrine sediments in the post rift section. This section was deposited as the extensional tectonic regime ceased. This makes the overall thickness approximately 100 ft thick. The formation is comprised of sand with occasional variable shale streaks. Many reservoirs were discovered in this formation. The UG Massive formation is the main target of exploration in Javaz field.

2.4.4 Trap

The Javaz Field is an inverted NE-SW four-way dip structure limited by a major reverse fault to the south. The movement of the thrust fault to the south caused inversion of the structure and formation of the anticline during the Oligo-Miocene. In West Natuna Basin, there are three types of traps, structural, stratigraphic, and combination between structural and stratigraphic. Anticlines are characterized as structural traps. Stratigraphic traps are associated with lateral or vertical changes in rock type and occur at pinch-outs, channel margins, or unconformities.

2.4.5 Seal

The primary seal in the Javaz field is the Slamet formation. Sediment in this formation was deposited in a lacustrine environment with a primary lithology of shale. The Slamet shale is extensively deposited over the entire area, and provides regional shale for underlying reservoirs throughout the Block B PSC area.

CHAPTER 3
THEORITICAL BACKGROUND

3.1 Seismic Reflection Theory

Propagation of waves through the earth is the fundamental basis of the seismic exploration method. Wave propagation depends on the elastic properties of the rocks and the fluids contained within them. Elastic properties can be described as how the rocks resist changes in size or shape when external forces are applied. The variation of how the rocks resist the changes are captured and interpreted as geological structure, lithology and fluid trough the travel time, phase, frequency and amplitude domains.

The ability of the rock to pass elastic wave is referred to as the acoustic impedance. Acoustic impedance is function of velocity and density. By measuring the acoustic impedance of the reflection events, we can measure the rocks resistance to changes in size and shape.

Seismic reflections will be formed if there is a change in acoustic impedance (AI) which is a function of velocity (V) and density (ρ) of the rock.

$$AI = \rho.V \qquad\qquad (3.1)$$

where:

AI = Acoustic Impedance

ρ *= Density (g/cm^3)*

V = Velocity (m/s)

When a seismic wave propagate through the ground and encounters the boundary between two media with different acoustic impedance at perpendicular incidence, some of energy will be reflected and measured as reflection coefficient, which can be expressed with equation below:

$$r_i = \frac{\rho_{i+1}V_{i+1} - \rho_i V_i}{\rho_{i+1}V_{i+1} + \rho_i V_i}$$

(3.2)

where:

ρ_i = density of layer i^{th}

V_i = velocity of layer i^{th}

Reflection coefficient from equation above (3.2), has value between -1 and 1, if acoustic impedance from the second media $\rho_{i+1}V_{i+1}$ is greater than acoustic impedance from the first media $\rho_i V_i$, the seismic wave propagate from low value of density-velocity to higher value of density-velocity, then the reflection coefficient value will be positive.

3.1.1 Seismic Trace

The basic model of seismic trace is referred to convolution model which is stated that every trace is result of convolution from reflectivity with seismic source and adds with noise (Russell, 1996). This convolution can be written as:

$$s_{(t)} = w_{(t)} * r_{(t)} + n_{(t)}$$

(3.3)

where:

$s_{(t)}$: Seismic Trace

$r_{(t)}$: Coefficient Reflection

$w_{(t)}$: Seismic wavelet

$n_{(t)}$: Noise

$*$: Convolution

3.1.2 P-wave velocity and S-wave velocity

Seismic waves are called elastic waves, because the oscillation of medium particles happens as a result of interaction between the stress gradient against elastic forces (Suprajitno, 2000). As shown in this picture below Figure 3.1 when a compressional wave is applied to a unit of rock it will change the volume and shape of the rock. When a shear wave is applied, it will only change the shape.
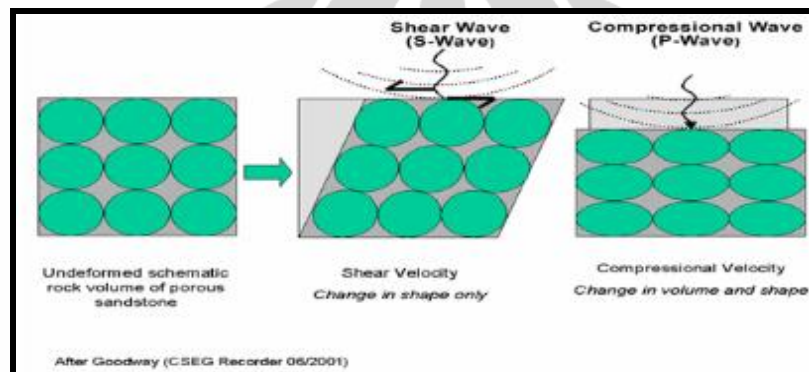
Figure 3.1 Rock deformation schemas against compressional wave (P-wave) and shear wave (S-wave), (Goodway, 2001)

Seismic wave velocity can be categorized based on how the wave travels and propagates. There are two types of waves. With a longitudinal wave, the oscillation of the particles in the medium is in line with propagation direction. This type of wave is also called a compressional wave or P-wave. ThiS-wave will arrive earlier compare to the other type of wave. The other wave is called Transversal wave, where the oscillation of the particles in the medium is perpendicular to the propagation direction. This is also called a rotational wave or shear wave. Hence it is called as S-wave. S-waves travel slower and will arrive after P-waves.

Relationship between P-wave (Vp) and S-wave (Vs) can be expressed as:

$$Vp = \sqrt{\frac{\lambda + 2\mu}{\rho}} = \sqrt{\frac{K + \frac{4}{3}\mu}{\rho}} \qquad (3.4)$$

$$Vs = \sqrt{\frac{\mu}{\rho}} \qquad (3.5)$$

Where:

λ = Lambda coefficient = $K + \frac{2}{3}\mu$

K = Bulk modulus

μ = Shear modulus

ρ = Density
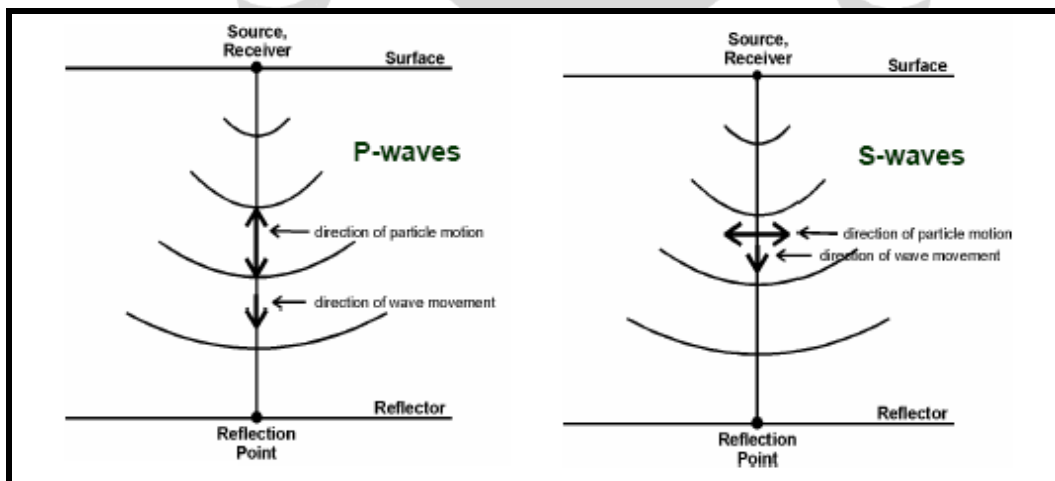
Figure 3.2 Showing particle motions against wave movements of P-waves and S-waves (Russel, 1999).

University of Indonesia

Ratio between Vp and Vs can be represented using *Poisson ratio* (σ) as:

$$\sigma = \frac{\gamma - 2}{2\gamma - 2} \qquad (3.6)$$

where: $\gamma = \left(\frac{Vp}{Vs}\right)^2 \qquad (3.7)$

Castagna (1985) derived empirical relationship of Vp and Vs for water-saturated clastic silicate rock, known as Mudrock Line..

$$Vp = 1.36 + 1.16Vs(km/s) \qquad (3.8)$$
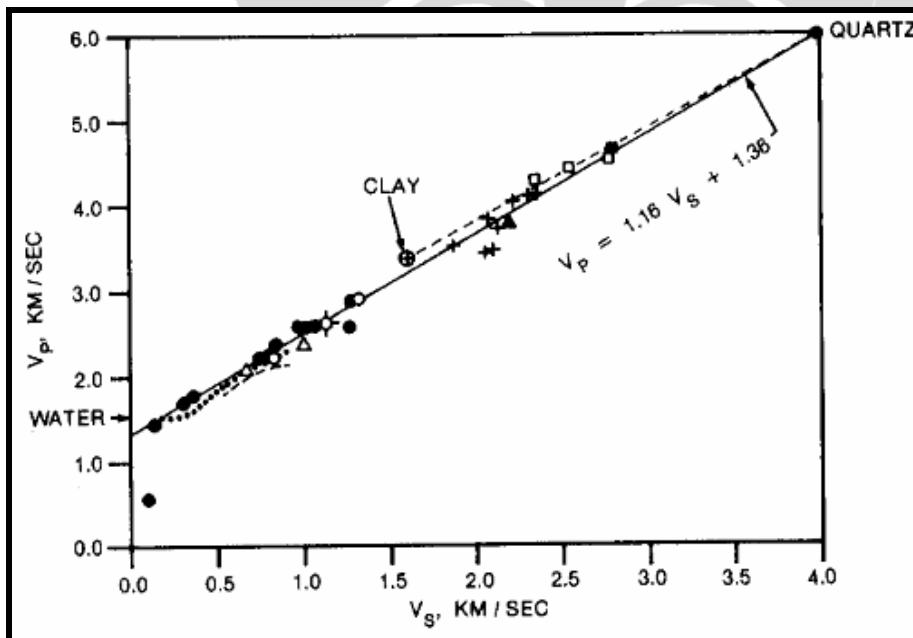
Figure 3.3 Mudrock Line. Relation between Vp and Vs (Russel, 1999)

The mudrock line can be used to calculate Vs however; this relation has a weakness, where the value of Vs is underestimated for soft consolidated sands and some clean sands. Thus mudrock line is valid only for water-saturated clastic silicate rock.

It is already known that Vp/Vs can be used as a lithology indicator. It can also be used as an indicator of isotropic parameters. For example, clay can have a higher Vp/Vs ratio than sandstone. In carbonates Vp/Vs can also be used to discriminate between dolomite and limestone. Vp/Vs through AVO method can also be used as DHI (Direct Hydrocarbon Indicator) since Vs is not sensitive to fluid while Vp is sensitive to both changes in lithology or fluid, hence Vp/Vs is a function of lithology and fluid changes.

3.2 Rock Physics

Rock physics is a bridge to link seismic, geological and reservoir properties. It can be used to describe condition of reservoir rock such as porosity, density, rigidity and incompressibility. The rock physics properties will tell us how seismic waves physically travel through the rocks, then this information can be used to describe geological and reservoir properties.

3.2.1 Porosity

Porosity is ratio between rock pore volume and total volume. This ratio can be represented in percent (%) or fraction, which then can be formulated as:

Porosity (ϕ) = (Pore volume/ Total volume) x 100% (3.9)

Effective porosity describes the amount of the total porosity that is connected and had been corrected to account for clay content. The value of effective porosity is smaller than total porosity.

University of Indonesia

3.2.2 Density

In simple way density is ratio between mass (Kg) to volume (m^3). Density is a parameter which is used in equation P-wave, S-wave, and acoustic impedance, where is all will give impact on how subsurface seismic wave responds. This density effect can be modeled into Wyllie equation:

$$\rho_{sat} = \rho_m \left(1 - \phi\right) + \rho_w S_w \phi + \rho_{hc} \left(1 - S_w\right)\phi \qquad (3.10)$$

where:

ρb = bulk density $\qquad\qquad$ ρm = matrix density

ρf = fluid density $\qquad\qquad$ ϕ = porosity

Sw = water saturation $\qquad\qquad$ ρw = water density (close to 1 g/cm^3)

ρhc = hydrocarbon density

Figure 3.4 describes that density reservoir rock dramatically drop in gas reservoir compare to oil reservoir. This characteristic is very important for seismic interpretation in a reservoir.
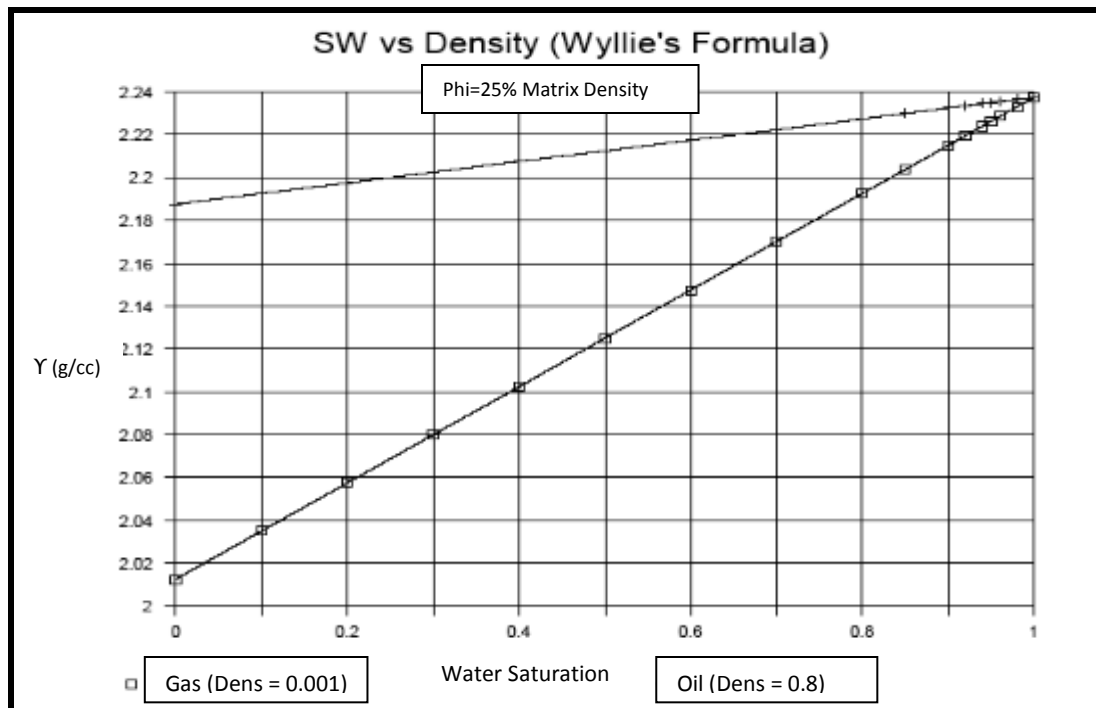
Figure 3.4 SW vs Density shows behaviour of gas and oil based on Wyllie's equation (Russel, 1999).

3.2.3 Rigidity ($\mu\rho$) and Incompressibility ($\lambda\rho$)

Rigidity or Mu-rho ($\mu\rho$) can be defined as how the material deforms when stress is applied. Rigidity is sensitive to the rock's matrix and not influenced by fluid therefore it can be used as lithology indicator. Low rigidity value will respond for coals and/or shales while sands or carbonates will showed by high value.

Incompressibility or Lambda-rho ($\lambda\rho$) is defined as the amount the volume of a material changes when stress is applied. The less volume changes when stress is applied, the higher the incompressibility and vise versa. Incompressibility measurements are dominated by changes in pore space in the rock as opposed to grain size. Because of this, Lamda-rho can be used as an indicator for both lithology and pore fluid. Low incompressibility values are associated with gas sand (Goodway et al., 1997).

Table 3.1 shows elastic properties of shale and gas sand. It suggests that Lambda-rho ($\lambda\rho$) is the most sensitive parameter showing rock properties changes from shale to gas sand.

Table 3.1 Rock physics analysis using Lame's parameter (Goodway et al., 1997).

TABLE 1	Vp (m/s)	Vs (m/s)	ρ (g/cc)	Vp/Vs	(Vp/Vs)²	σ	λ + 2μ	μ	λ	λ/μ
Shale	2898	1290	2.425	2.25	5.1	0.38	20.37	4.035	12.3	3.1
Gas Sand	2857	1666	2.275	1.71	2.9	0.24	18.53	6.314	5.9	0.9
Avg. Change	1.40%	25%	6.40%	27%	55%	45%	9.20%	44%	70%	110%

(moduli λ, μ are in GPa's)

Based on equations (3.4) and (3.5), Vp and Vs parameter can be transformed into another physical parameter Rigidity and Incompressibility as follow as:

$$Vp = \sqrt{\frac{\lambda + 2\mu}{\rho}} \quad \text{And} \quad Vs = \sqrt{\frac{\mu}{\rho}}$$

so,

$$Z_s^2 = (\rho Vs)^2 = \mu\rho = \text{Mu-rho (Rigidity)} \tag{3.11}$$

and,

$$Z_P^2 = (\rho Vp)^2 = (\lambda + 2\mu)\rho \tag{3.12}$$

then,

$$\lambda\rho = Z_p^2 - 2Z_s^2 = \text{Lambda-rho (Incompressibility)} \tag{3.13}$$

3.3 Amplitude Variation with Offset (AVO)

When seismic data is acquired, multiple source-receiver pairs will sample the same point in the subsurface. Each distance from source to receiver (offset) is related

to a different angle of incidence at a reflection point. The larger the offset, the greater the incident angle. The principle behind AVO analysis is that the changes of amplitude observed with increasing offset or incidence angel can be related to rock properties or the fluid content of a reservoir. For example, increasing amplitude with increasing offset could be related to the presence of gas in a reservoir. Primarily, the AVO effects can be related to lithologic or rock property effects; however, fluid effects can also cause changes in AVO.

Originally, the AVO method was used as a technique to validate amplitude anomaly in seismic that related to gas presence in a reservoir (Ostrander, 1982). This anomaly would be represented as a reflection of higher amplitude than the surrounding reflections. This phenomena anomaly is called a "bright spot". Unfortunately, not all bright spots are the result of gas since coal, porous zones, salt, conglomerate, turbidite and tuning effect of thin lamination can also give the same result (Pendrel et al., 2000). Because of this, the AVO method was further developed to reduce this uncertainty.

Energy partitioning will cause AVO at a surface of reflector. When a seismic wave encounters a reflection boundary, some of the energy is reflected and some of the energy is transmitted deeper into the subsurface. When the angle of incidence is greater than zero, P-wave energy is partitioned and transmitted to become P and S components and the amplitudes of both the reflected and transmitted energy depend on the contrast in rock physics properties across the surface reflector. The rock physics properties that control these effects include compressional wave velocity (Vp), shear wave velocity (Vs), density (ρ) and the angle-of-incidence. It can be illustrated as in Figure 3.5 below:
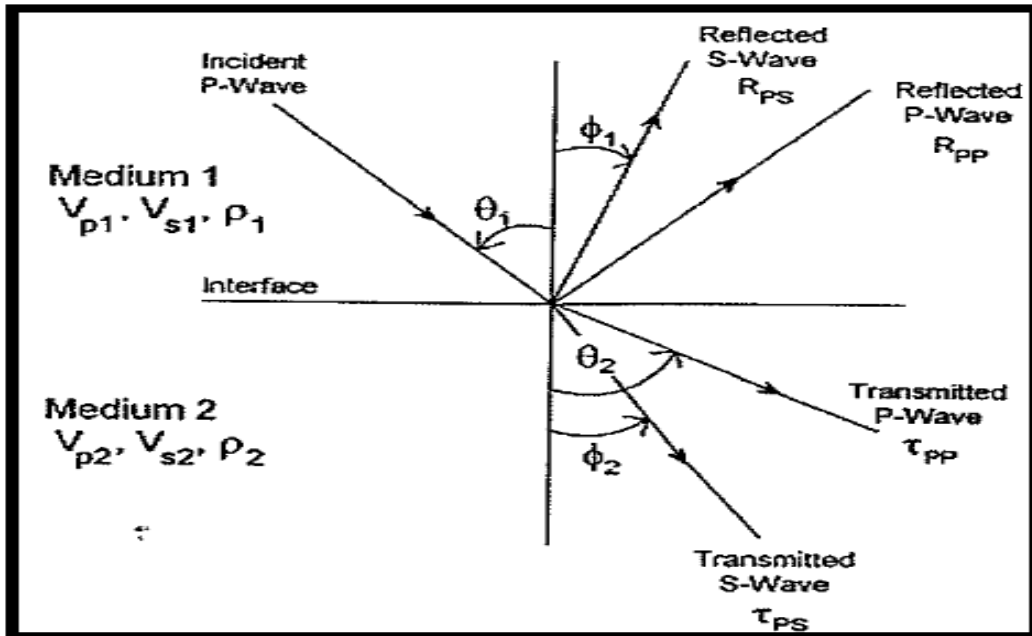
University of Indonesia

Figure 3.5 Wave energy reflections at surface boundary (Russel, 1999)

This phenomenon (AVO) in early 20th century was formulated within four equations with four unknowns by Karl Zoeppritz, where incident P-wave hitting the boundary between two layers will produce reflected and refracted waves as the function of Vp, Vs and ρ. The formula is:

$$
\begin{bmatrix} R_p(\theta_1) \\ R_s(\theta_1) \\ T_p(\theta_1) \\ T_s(\theta_1) \end{bmatrix} = \begin{bmatrix} -\sin\theta_1 & -\cos\phi_1 & \sin\theta_2 & \cos\theta_2 \\ \cos\theta_1 & -\sin\phi_1 & \cos\theta_2 & -\sin\phi_2 \\ \sin 2\theta_1 & \dfrac{Vp_1}{Vs_1}\cos 2\phi_1 & \dfrac{\rho_2 V_{s2}^2 V_{p1}}{\rho_1 V_{s1}^2 V_{p1}}\cos 2\phi_1 & \dfrac{\rho_2 V_{s2}V_{p1}}{\rho_1 V_{S1}^2}\cos 2\phi_2 \\ -\cos 2\phi_1 & \dfrac{Vs_1}{Vp_1}\sin 2\phi 1 & \dfrac{\rho_2 V_{p2}}{\rho_1 V_{p1}}\cos 2\phi 2 & \dfrac{\rho_2 V_{s2}}{\rho_1 V_{p1}}\sin 2\phi 2 \end{bmatrix}^{-1} \begin{bmatrix} \sin\theta_1 \\ \cos\theta_1 \\ \sin 2\theta_1 \\ \cos 2\phi_1 \end{bmatrix} \quad (3.14)
$$

where:

R_P, R_S, T_P, and T_S, are the reflected P, reflected S, transmitted P, and transmitted S-wave amplitude coefficients, Vp is P-wave velocity, Vs is S-wave velocity and ρ is density.

This Zoeppritz formula is very complicated to solve. Aki-Richard and Frasier then approximated this equation into 3 terms.

$$R(\theta) = W - X \sin^2 \theta + Y \frac{1}{\cos^2 \theta_{avg}} - Z \sin^2 \theta \qquad (3.15)$$

where:

$$W = \frac{1}{2}\frac{\Delta\rho}{\rho}; \quad X = 2\frac{V_s^2}{V_{p1}^2}\frac{\Delta\rho}{\rho}; \quad Y = \frac{1}{2}\frac{\Delta V_p^2}{V_p^2}; \quad Z = 4\frac{V_s^2}{V_{p1}^2}\frac{\Delta V_s^2}{V_s^2}$$

and "delta (Δ)" is like example below:

$$\frac{\Delta\rho}{\rho} = \frac{\rho_2 - \rho_1}{(\rho_1 + \rho_2)/2}$$

Adapted from (Avseth et.al, 2006).

In 1985 this Zoepprits formulas was simplified by Shuey, became:

$$R(\theta) = R(0) + G\sin^2\theta + F(\tan^2\theta - \sin^2\theta) \qquad (3.16)$$

where:

$$R(0) = \frac{1}{2}\left(\frac{\Delta V_p}{V_p} + \frac{\Delta\rho}{\rho}\right); \quad G = \frac{1}{2}\frac{\Delta V_p}{V_p} - 2\frac{V_s^2}{V_p^2}\left(\frac{\Delta\rho}{\rho} + 2\frac{\Delta V_s}{V_s}\right); \quad F = \frac{1}{2}\frac{\Delta V_p}{V_p}$$

Adapted from (Avseth et.al, 2006).

From the final result can be concluded that AVO responds is strongly influenced by $R(0)$ at low angles and influenced by G at higher angles. Qualitative AVO analysis is done on common-mid-point-gathers. Each amplitude values from each offset gather are collected and regressed linearly to determine the relation between amplitude and offset. The primary attributes used to describe AVO responses are Intercept and Gradient. The Intercept is defined as the amplitude measured when angle is zero (normal incidence) and the Gradient describes the change in amplitude as angle increases. .

Conversion from offset distance to angle of incidence is required since seismic recorded is done by offset distance while the equations above are function of incidence angel. Figure 3.6 and Figure 3.7 illustrate AVO (offset) and AVA (angle).
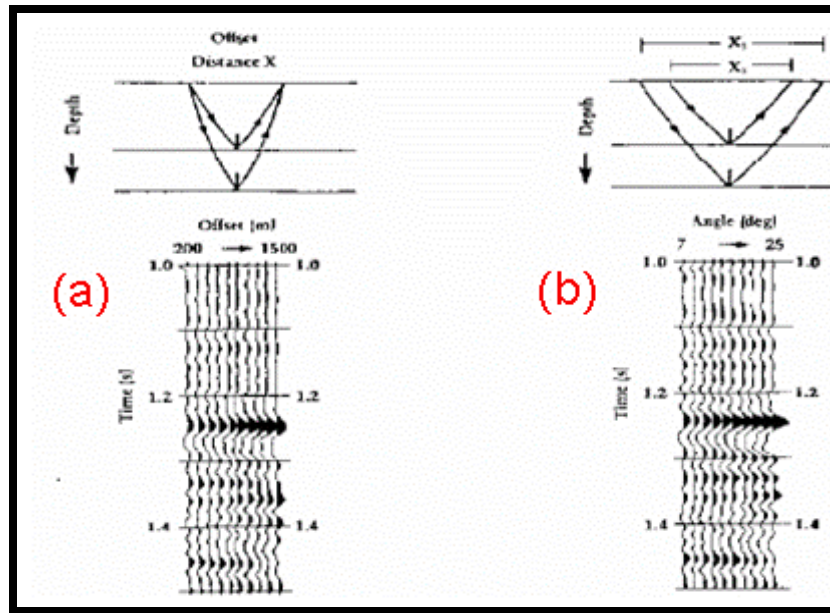

Figure 3.6 Showing AVO response (a) and transformation to AVA (b) (Russel, 1999)
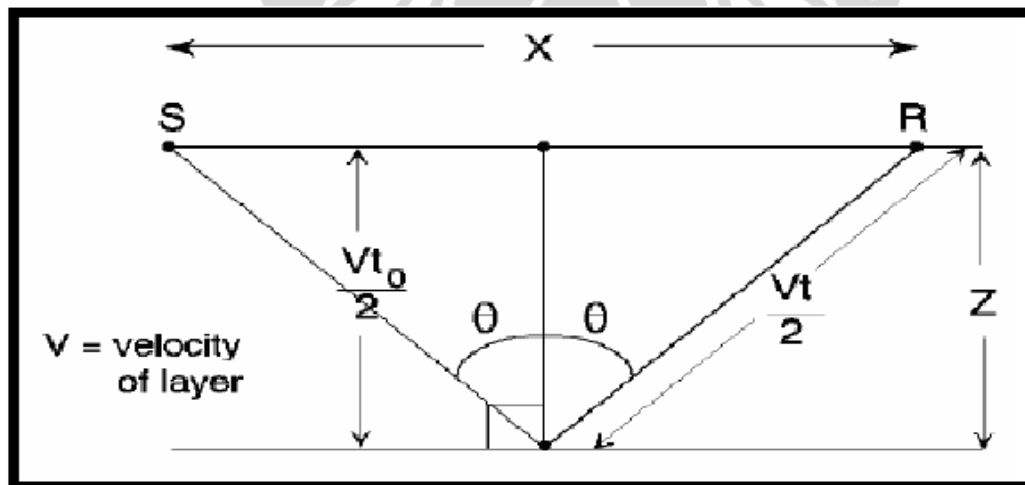

Figure 3.7 Seismic wave tracks from source to receiver with constant velocity (Russel, 1999)

The relationship between offset and angle can show as:

$$\tan\theta = x/2z \qquad (3.17)$$

where:

θ = angle

x = offset

z = depth

If velocity of the media is known, the equation will be:

$$Z = V.t_o / 2 \qquad (3.18)$$

where:

V = velocity (RMS or average)

T = time at zero-offset

By substituting equation (3.18) into (3.17), we will get :

$$\tan\theta = x / V.t_o \qquad (3.19)$$

then,

$$\tan\theta = x / V.t_o \qquad (3.20)$$

Using this equation, the offset function can be changed into an angle function. AVO analysis is only valid up to the critical angle (angle which gives rise to a critically refracted ray that travels along the reflection interface). At angles higher than the critical angle, the behavior of the signal reflections will not follow normal behaviors for AVO analysis.

Characterization of different types of responses depending on lithology and fluid type has become the basis for the use of the AVO plot in interpretation. The first classification shale/brine sand AVA responses was classified by Rutherford and Williams in 1989 into three types (I, II & III) depending on the impedance contrast between the shale and the sand (opcite Sukmono, 2002). Class-1 is high impedance gas-sandstone; Class-2 is near zero contrast gas-sandstone; Class-3 is low impedance gas sandstone. In 1995 Ross and Kinman have suggested that the small positive Class-2 response should be termed Class-2p, owing to the phase reversal that is

inherent in this response. A further class of AVO type (IV) was introduced by Castagna and Swan (1997). This response has a strong negative reflection coefficient with decreasing amplitude with angle.

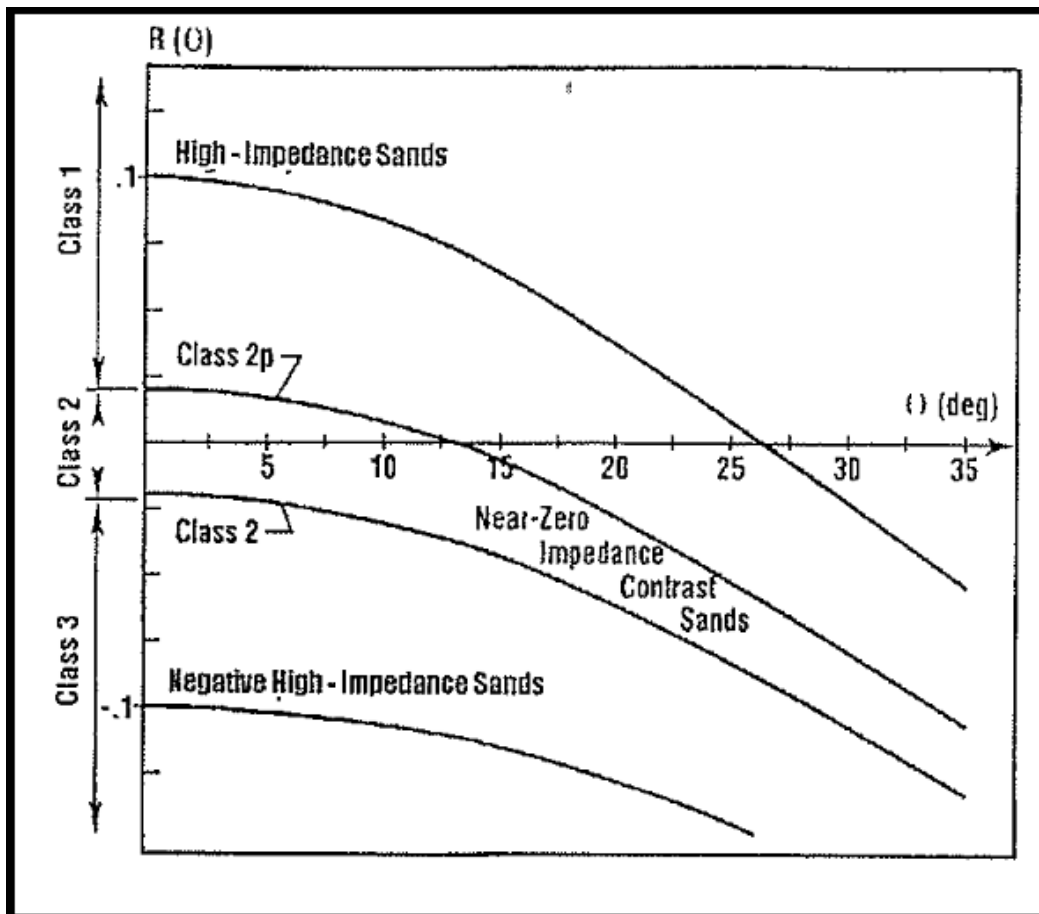Figure 3.8 Anomaly amplitude classification based on Rutherford and Williams (1989) and Castagna and Swan (1997)

3.4 Seismic Inversion

Seismic inversion can be defined as a subsurface geological modeling technique using seismic data as input and well log as the control (Sukmono, 2002). This is accomplished through a process of transforming seismic amplitude value into impedance value.

University of Indonesia

In geophysical modeling there are two primary types of modeling, Forward modeling and Inverse modeling. Forward modeling is predicting a geophysical response from an earth model while Inverse modeling is predicting an earth model from a geophysical response.
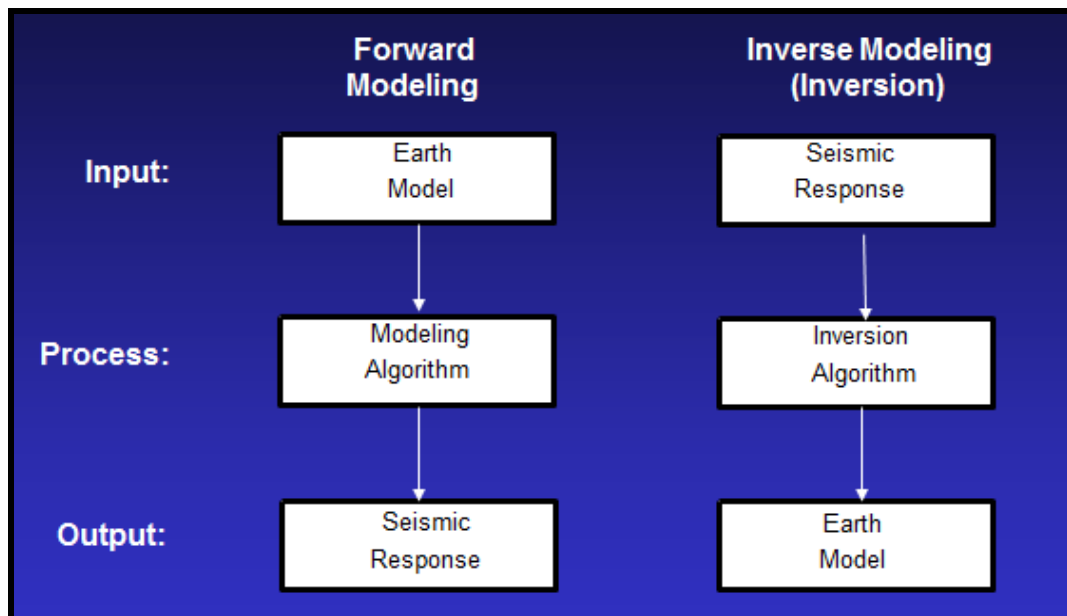

Figure 3.9 Forward and Inverse Modeling (Russel, 1999)

There are numerous advantages of using seismic inversion method, such as:
- Acoustic impedance data shows the layers in the subsurface which makes it easier to visualize.
- It's easier to define top and bottom of rock layers or even stratigraphy feature.
- Reduce wavelet effect, decrease sides lobe and tuning effect causing by thin layer.
- Can be quantitatively to predict reservoir.

In seismic inversion method we are dealing with two types of seismic data, they are Pre-stack seismic and Post-stack seismic data. Post-stack seismic data produce only AI (Zp) it is because seismic amplitude is only represented by $R_{(0)}$ while Pre-stack seismic data produce AI (Zp), SI (Zs), ρ and its derivative such as: Vp/Vs, Lamda-

rho, Mu-rho to predict the fluid and lithology properties from subsurface. The fundamental of seismic inversion model is based on 1-D convolution model, where seismic trace is a convolution of earth reflectivity and wavelet with some noise.

3.5 Seismic Simultaneous Inversion

There are multiple inversion algorithms available. The Elastic Impedance algorithm analyzes one or more angle stacks to derive non-physical "elastic impedance" and the Independent Inversion algorithm analyzes pre-stack gathers to derive acoustic impedance, shear impedance and density volumes independently. In Seismic Simultaneous Inversion, both pre-stack and post-stack seismic data are used. The pre-stack data is used to define the AVO response and try to infer fluid content while the post-stack data is inverted to derive an acoustic impedance volume. Using this algorithm, pre-stack gathers or angle stacks are analyzed to derive acoustic impedance, shear impedance and density volumes simultaneously. In this thesis, the Simultaneous Inversion algorithm from Hampson- Russel is used. This theory has been published by Hampson et al in 2005 at SEG/Houston annual meeting and the algorithm is based on three assumptions:

- The linearized approximation for reflectivity holds
- PP and PS reflectivity as a function of angel can be given by Aki-Richard equations (Aki and Richards, 2002)
- Linear relationship between the logarithm of P-impedance and both S-impedance and density.

This algorithm is extended the work of Simmons and Backus (2003) and Buland and Omre (1996), and build a new approach to invert directly for P-impedance ($Zp = \rho Vp$), S-impedance ($Zs = \rho Vs$) and density. Simmons and Backus (2003) using equation below to invert for linearized all the reflectivity, where

$$Rp = \frac{1}{2}\left[\frac{\Delta V_p}{V_p} + \frac{\Delta \rho}{\rho}\right]$$ (3.21)

$$Rs = \frac{1}{2}\left[\frac{\Delta V_s}{V_s} + \frac{\Delta \rho}{\rho}\right] \tag{3.22}$$

$$R_D = \frac{\Delta \rho}{\rho} \tag{3.23}$$

These three equations above can be estimate from the angle dependent reflectivity $R_{pp}(\theta)$ using Aki-Richard linearized approximation. From Gardners relationship V_p and ρ can be used from equation

$$\frac{\Delta \rho}{\rho} = \frac{1}{4}\frac{\Delta V_p}{V_p} \tag{3.24}$$

And from the Castagna equation (Castagna et al., 1985), given by

$$V_s = (V_p - 1360)/1.16 \tag{3.25}$$

Bulan and Omre (2003) using three terms to parameterized $\frac{\Delta V_p}{V_p}$, $\frac{\Delta V_s}{V_s}$ and

$\frac{\Delta \rho}{\rho}$ against Aki-Richard approximation, and then Hampson Russel for changes in P-wave is used

$$\frac{\Delta V_p}{V_p} \approx \Delta \ln V_p \tag{3.26}$$

Where ln is natural logarithm.

Before the process continues we will review the model-based post-stack inversion by combining equation (3.21) and (3.26) small reflection of P-wave reflectivity can be given as

$$R_{pi} \approx \frac{1}{2}\Delta \ln Z_{pi} = \frac{1}{2}\left[\ln Z_{pi+1} - \ln Z_{pi}\right] \tag{3.27}$$

Where i is the interface between layer i and i+1, if we consider equation (3.27) above as N sample then the equation can be written in matrix as below

$$
\begin{bmatrix} R_{P1} \\ R_{P2} \\ \vdots \\ R_{PN} \end{bmatrix} = \frac{1}{2} \begin{bmatrix} -1 & 1 & 0 & \cdots \\ 0 & -1 & 1 & \ddots \\ 0 & 0 & -1 & \ddots \\ \vdots & \ddots & \ddots & \ddots \end{bmatrix} \begin{bmatrix} L_{P1} \\ L_{P2} \\ \vdots \\ L_{PN} \end{bmatrix} \qquad (3.28)
$$

where $L_{pi} = \ln(Z_{pi})$

Then the seismic trace as the convolution of wavelet and reflectivity from the earth, can be written in the matrix as below

$$
\begin{bmatrix} T_1 \\ T_2 \\ \vdots \\ T_N \end{bmatrix} = \begin{bmatrix} w_1 & 0 & 0 & \cdots \\ w_2 & w_1 & 0 & \ddots \\ w_3 & w_2 & w_1 & \ddots \\ \vdots & \ddots & \ddots & \ddots \end{bmatrix} \begin{bmatrix} R_{P1} \\ R_{P2} \\ \vdots \\ R_{PN} \end{bmatrix} \qquad (3.29)
$$

where T = seismic trace

W = seismic wavelet

Combining equations from the matrix above (3.28) and (3.29), we can derive a forward model which relates to the seismic trace of P-impedance:

$$
T = (\tfrac{1}{2})WDL_P \qquad (3.30)
$$

where:

W = wavelet matrix given in equation (3.29)

D = derivative matrix given in equation (3.28)

To avoid instability problems and recover low frequencies in equation (3.30) it can be inverted using a standard matrix to estimate L_p from T and W and build an initial impedance model and conjugate gradient model.

Then Fatti et al (1994) re-formulate the Aki-Richard equation.

$$R_{pp}(\theta) = c_1 R_{p0} + c_2 R_{s0} + c_3 R_D \qquad (3.31)$$

where:

$$c_1 = 1 + \tan^2 \theta$$
$$c_2 = -8\gamma^2 \sin^2 \theta$$
$$c_3 = -\frac{1}{2}\tan^2 \theta + 2\gamma^2 \sin^2 \theta$$
$$\gamma = \frac{V_s}{V_p}$$

and

R_{pp} = total reflectivity R_p = P-wave reflectivity

R_s = S-wave reflectivity R_D = density reflectivity

V_p = P-wave velocity V_s = S-wave velocity

ρ = density

For angel trace $T(\theta)$ we can extend the zero offset trace given in equation (3.30) and combine with equation (3.31)

$$T(\theta) = (\tfrac{1}{2})c_1 W(\theta)DL_P + (\tfrac{1}{2})c_2 W(\theta)DL_s + W(\theta)c_3 DL_D \qquad (3.32)$$

where: $L_s = \ln(Z_s)$ and $L_D = \ln(\rho)$

Using equation (3.32) we can now use it for inversion since the wavelet is dependent on angle and is dealing with impedance rather than velocity. From this we get different relationship than Simmons and Backus (1996) as below

$$\ln(Z_s) = k\ln(Z_P) + k_c + \Delta L_s \tag{3.33}$$

and

$$\ln(Z_D) = m\ln(Z_P) + m_c + \Delta L_D \tag{3.34}$$

This deviation in linear fit can be illustrated in figure below
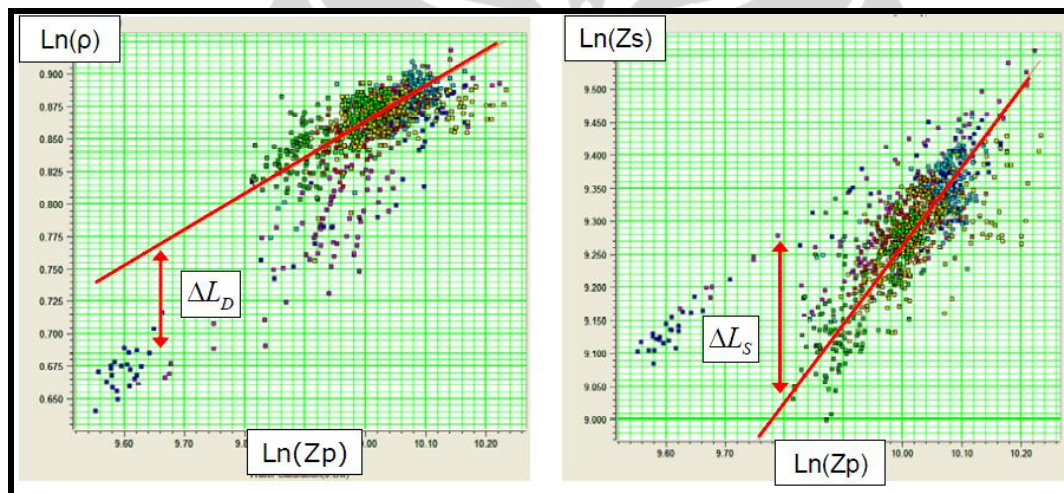

Figure 3.10 Crossplots of (a) $\ln(Z_D)$ vs $\ln(Z_P)$ and (b) $\ln(Z_s)$ vs $\ln(Z_P)$ where, in both cases, a best straight line fit has been added.

The next step is to combine equation (3.32), (3.33) and (3.34) will get

$$T(\theta) = \tilde{c}_1 W(\theta) DL_P + \tilde{c}_2 W(\theta) D\Delta L_s + W(\theta) c_3 D\Delta L_D \tag{3.35}$$

where: $\tilde{c}_1 = (\frac{1}{2})c_1 + (\frac{1}{2})kc_2 + mc_3$ and $\tilde{c}_2 = (\frac{1}{2})c_2$

Equation (3.35) can be write in the matrix as below

$$\begin{bmatrix} T(\theta_1) \\ T(\theta_2) \\ \vdots \\ T(\theta_N) \end{bmatrix} = \begin{bmatrix} \tilde{c}_1(\theta_1)W(\theta_1)D & \tilde{c}_2(\theta_1)W(\theta_1)D & c_3(\theta_1)W(\theta_1)D \\ \tilde{c}_1(\theta_2)W(\theta_2)D & \tilde{c}_2(\theta_2)W(\theta_2)D & c_3(\theta_2)W(\theta_2)D \\ \vdots & \vdots & \vdots \\ \tilde{c}_1(\theta_N)W(\theta_N)D & \tilde{c}_2(\theta_N)W(\theta_N)D & c_3(\theta_N)W(\theta_N)D \end{bmatrix} \begin{bmatrix} L_P \\ \Delta L_s \\ \Delta L_D \end{bmatrix} \qquad (3.36)$$

This matrix will solve the problem mentioned before about instability and low frequency loss, and to initialize the solution to

$$\begin{bmatrix} L_P & \Delta L_s & \Delta L_D \end{bmatrix}^T = \begin{bmatrix} \log(Z_{P0}) & 0 & 0 \end{bmatrix}^T \qquad (3.37)$$

Where Z_{P0} is the initial impedance model, and then using the conjugate gradient method, finally we can calculate of Z_P, Z_s and ρ.

$$Z_P = \exp(L_P) \qquad (3.38)$$

$$Z_s = \exp(kL_p + k_c + \Delta L_s) \qquad (3.39)$$

$$\rho = \exp(mL_p + m_c + \Delta L_D) \qquad (3.40)$$

CHAPTER 4

APPLICATION OF SIMULTANEOUS INVERSION TO 3D SEISMIC DATA

Data preparation is a very important step in the process of generating a successful inversion. Each input was prepared appropriately for this study. Figure 4.1 shows the workflow of the data input and inversion process. Well data required for the Simultaneous inversion method, especially Vp, Vs and check shot data. Seismic data used consisted of near, mid, far angle stack, and full stack data. All information was validated such as well header, directional survey; time-depth data, top markers, logs, seismic survey, etc., then loaded into the database application, in this study, HRS software.
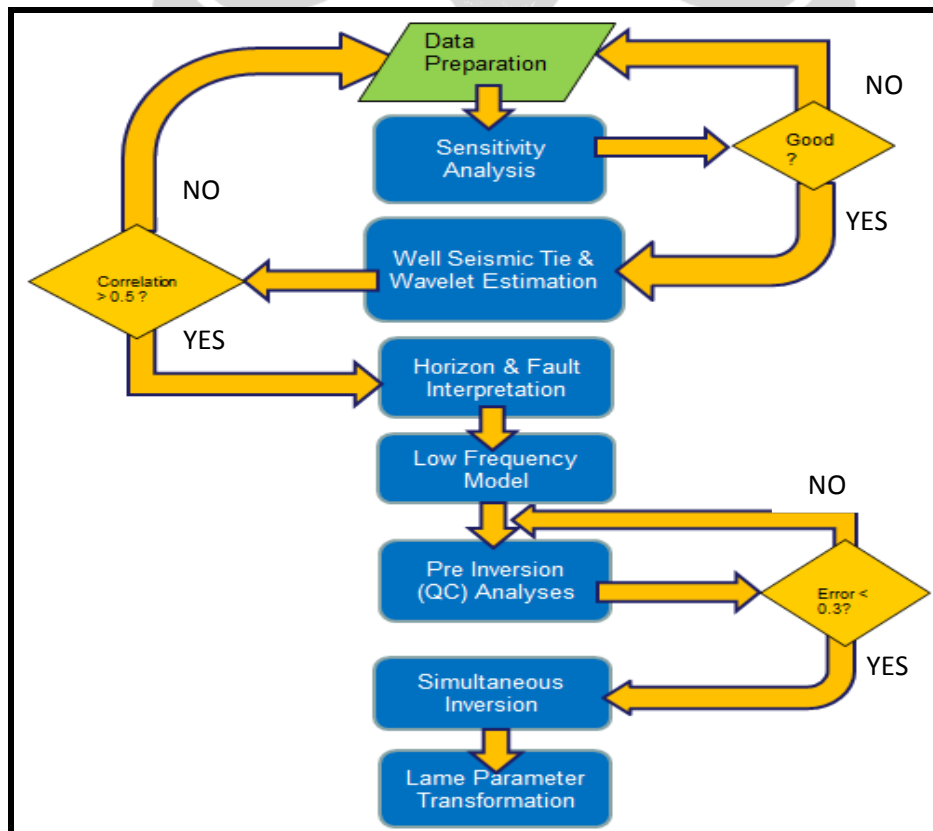

Figure 4.1 Thesis workflow

4.1 Well Data

There are 4 wells located in Javaz field, Javaz-1A, Javaz-2, Javaz-3 and Javaz-4. Figure 4.2 shows a well correlation of all four wells. The wells were drilled from 2000 – 2001. The Javaz-1A well was drilled to total depth of 6050 ft MDKB in the apex of western Javaz structure. The Javaz-2 well was drilled to total depth of 8864 ft MD, located approximately 700 meters southwest of Javaz-1A location. The Javaz-3 well was drilled to total depth of 6155 ft MD, located in the western part of west Javaz structure, approximately 2.5 km east of Javaz-2. The Lower UG is interpreted as a water bearing zone. The Javaz-4 well is located in the east Javaz structure, approximately 1 km north east from Javaz-1A location, drilled to total depth of 7,276 ft MDKB.

In this study only the Javaz-4 well was used, since this well has complete well logs and supporting data requirements. It also has the best correlation result.. The data required is checkshot or VSP, density, P-wave and S-wave logs. P-wave log is used to tie the well to seismic. S-wave log is used to derive Lame parameters (Lambda-rho, Mu-rho and Lambda per Mu). Other standard petrophysical logs such as Gamma Ray, Caliper, Resistivity, Neutron, Effective Porosity, Water Saturation, etc. were used for sensitivity analysis to determine reservoir properties. Figure 4.3 and 4.4 show Javaz-3 and Javaz-4 wells with zone of interest - UG massive formation.
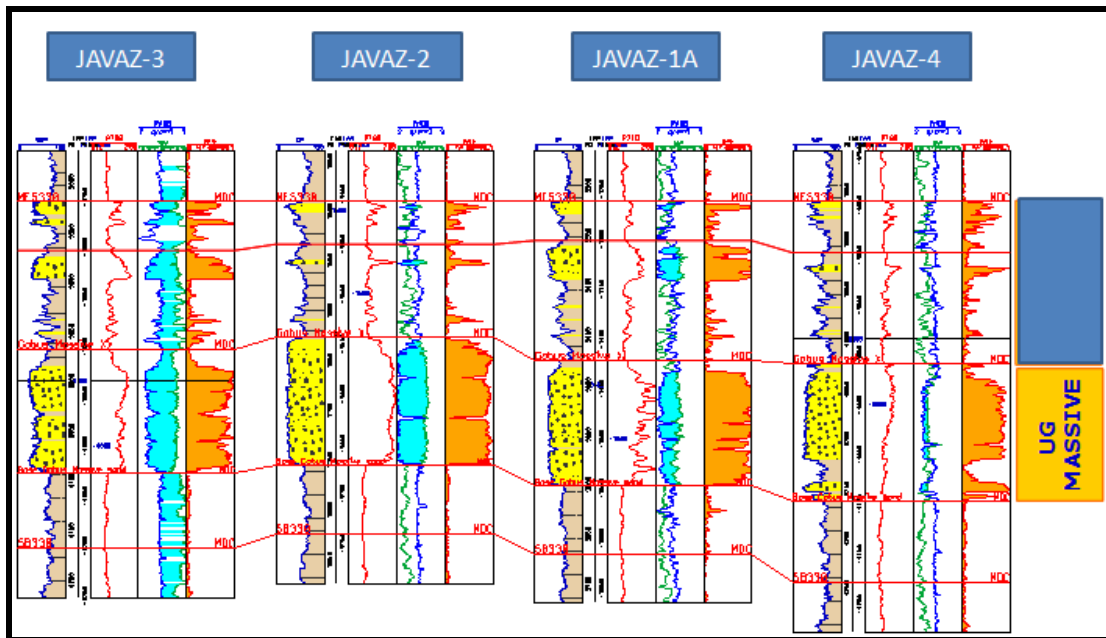
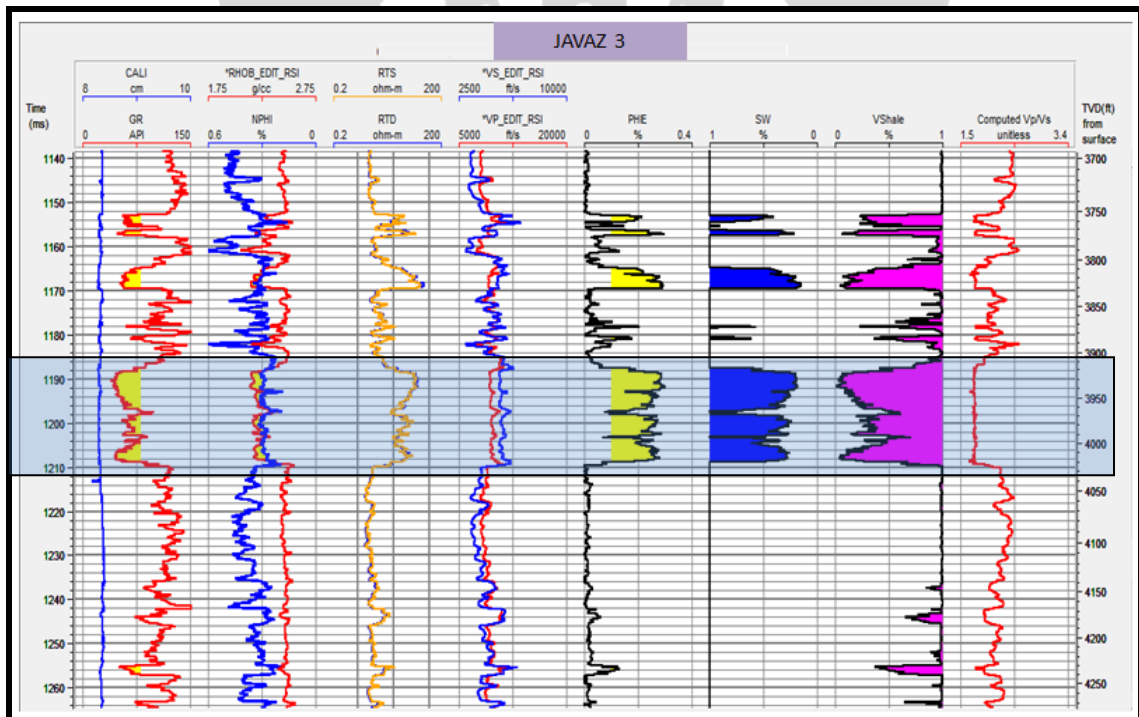Figure 4.2 Well correlation of Javaz wells (ConocoPhillips, 2006)

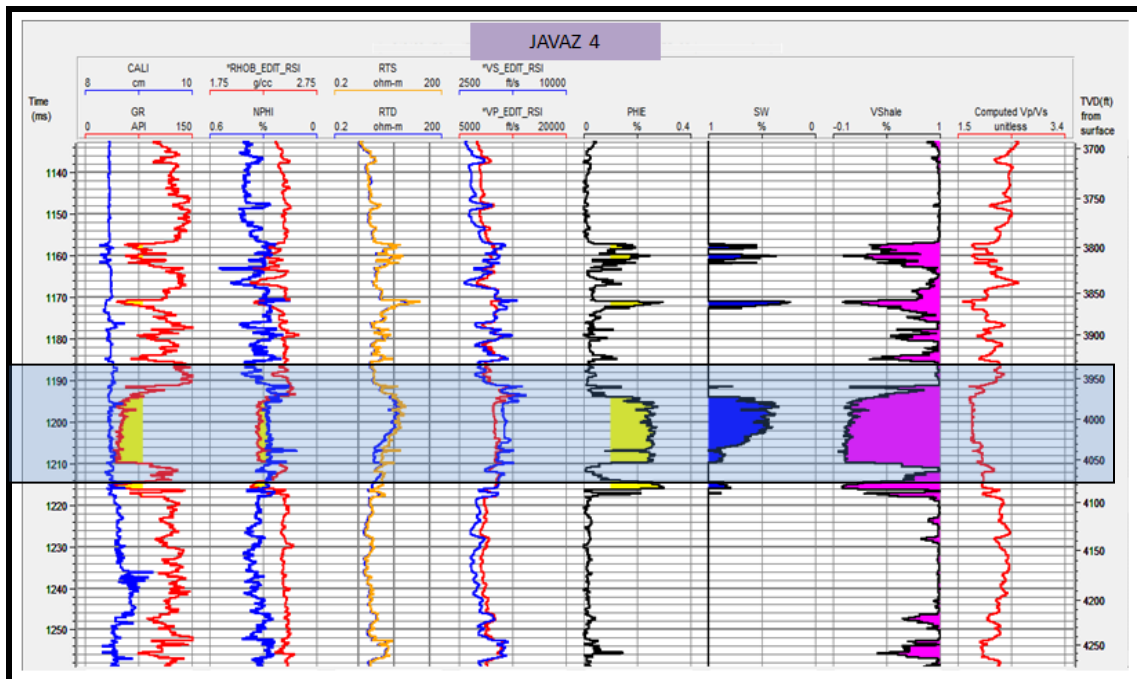Figure 4.3 Javaz-3 at the interested zone UG Massive formation

University of Indonesia

Figure 4.4 Javaz-4 at the interested zone UG Massive formation

4.2 3D Seismic Data

Seismic volumes consist of near stack ($5^{o}-15^{o}$), mid stack ($15^{o}-25^{o}$), far stack ($25^{o}-35^{o}$) and full stack data. The survey coverage is between Inline 6100 – 8000 and X-line 4100-4700. Prior to use, seismic volumes in this study have been proper conditioned for AVO and attribute analysis by processing company in 2005. A seismic section of full migrated stack data across Javaz-1A, Javaz-2, Javaz-3 and Javaz-4 wells are shown in Figure 4.5. Figure 4.6 shows a seismic section of Near, Mid and Far angle stack.
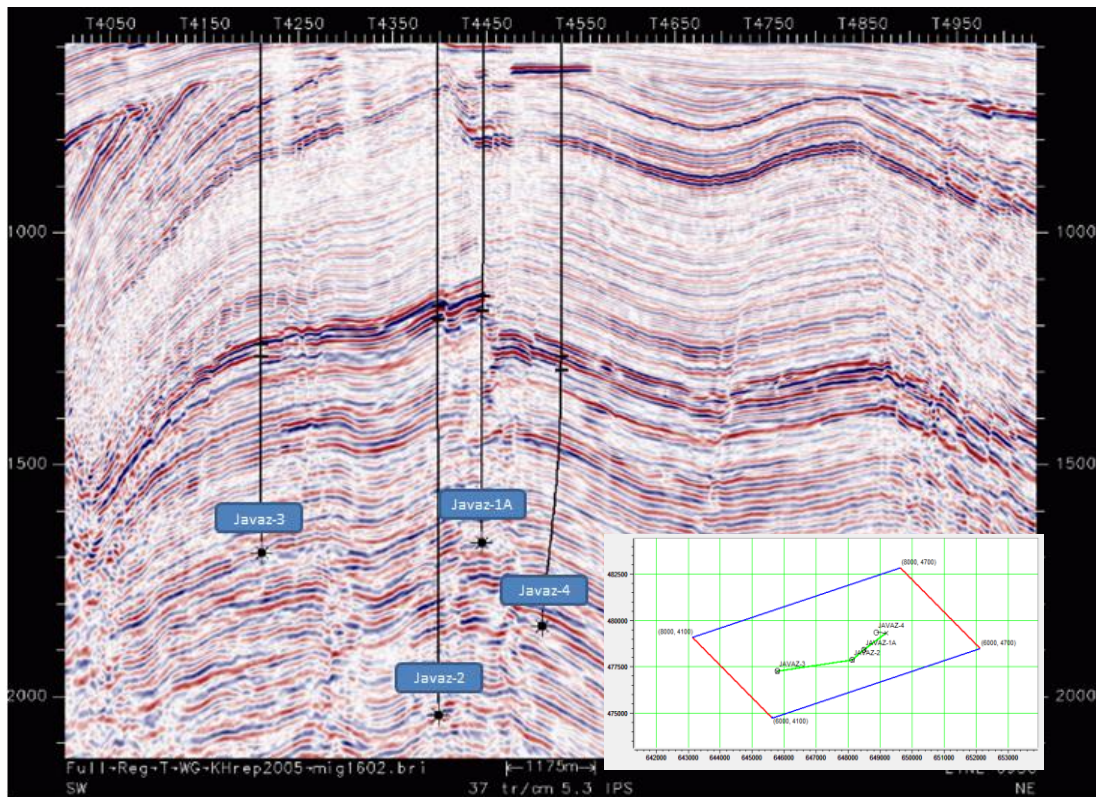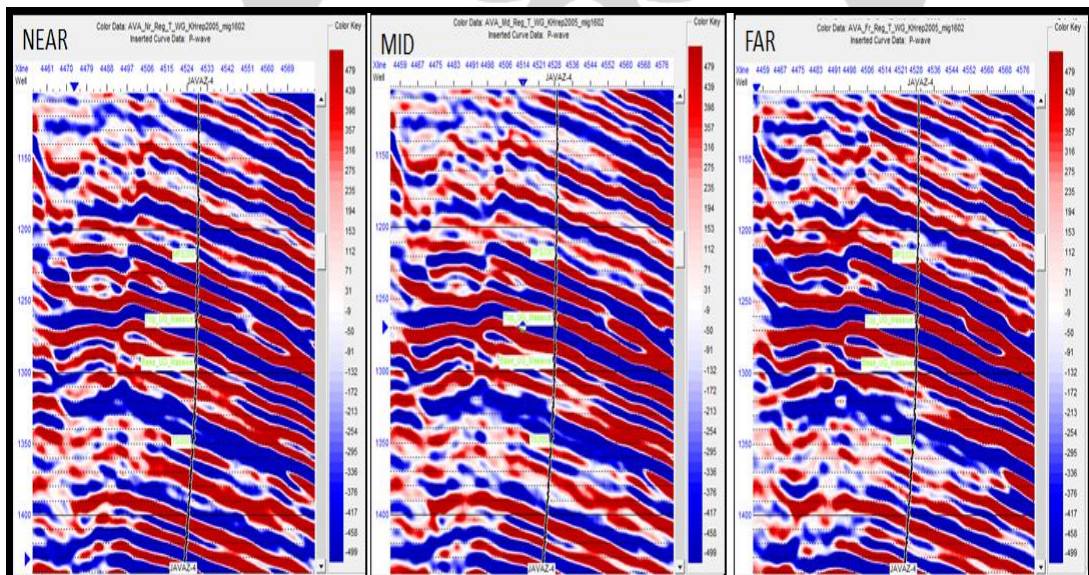
Figure 4.5 Full migrated stack at all well

Figure 4.6 Seismic sections near, mid and far at Javaz-4

4.3 Sensitivity Analysis

A sensitivity analysis is conducted to measure how much the data can be used to distinguish lithology and fluid content at the zone of interest. It can be done by cross-plotting elastic parameters of well logs. It required log data such as density, gamma ray, P-wave, S-wave, porosity, Vp/Vs, water saturation and derivative logs such as P-impedance, S-impedance, Lambda-rho, Mu-rho and lambda over mu. Prior to inversion, several elastic parameters were cross-plotted to determine which elastic parameters were sensitive to lithology and fluid changes. Figure 4.7 showed relationship between P-impedance and S-impedance where low and high water saturation can be distinguished very well.
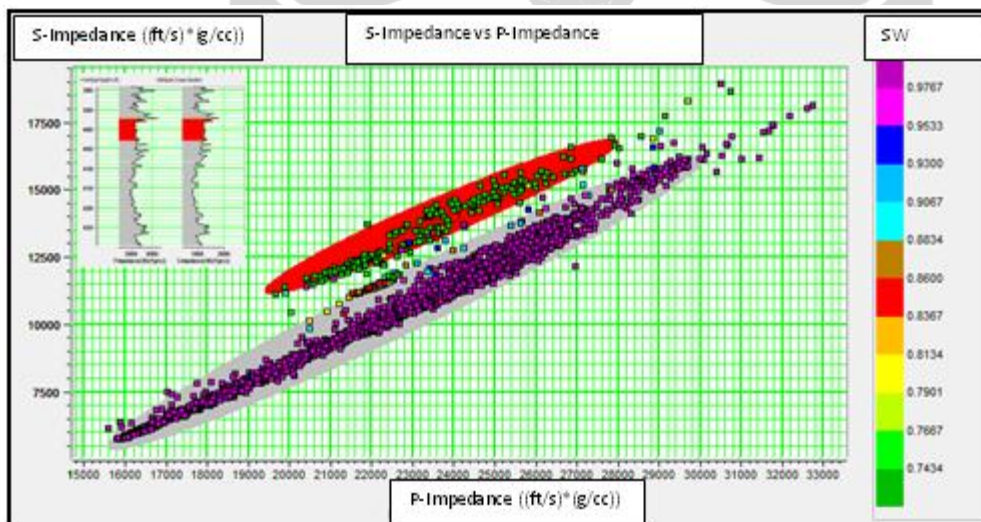

Figure 4.7 Cross plot between P-impedance and S-impedance, red color shows low water saturation content.

Figure.4.8 shows a cross-plot of porosity and density with water saturation as the color bar (third axis). The result suggests that high gamma ray (purple dot color) correlates well with low porosity and low gammy ray (green dot color) correlates well with high porosity. In other word, by looking at porosity and density relationship, we can distinguish gas sand and shale.
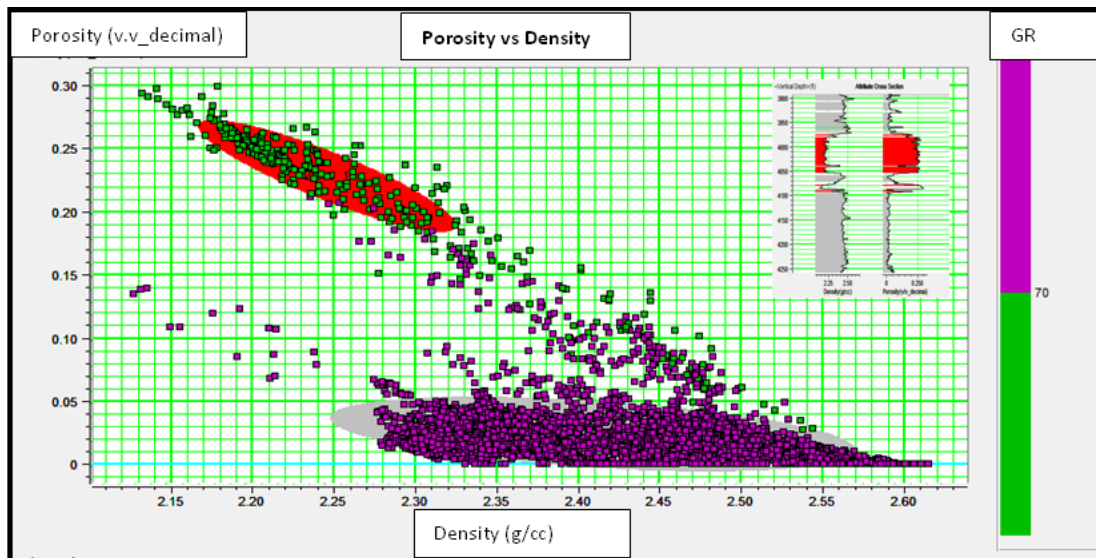
Figure 4.8 Cross plot porosity and density with gamma ray cut of at 70

Goodway (1997) showed lambda over mu was the most sensitive elastic parameter to distinguish gas sand and shale (Table 4.1). Figure 4.9 also suggested large separation between gas sand and shale was shown by lambda over mu cross-plot.
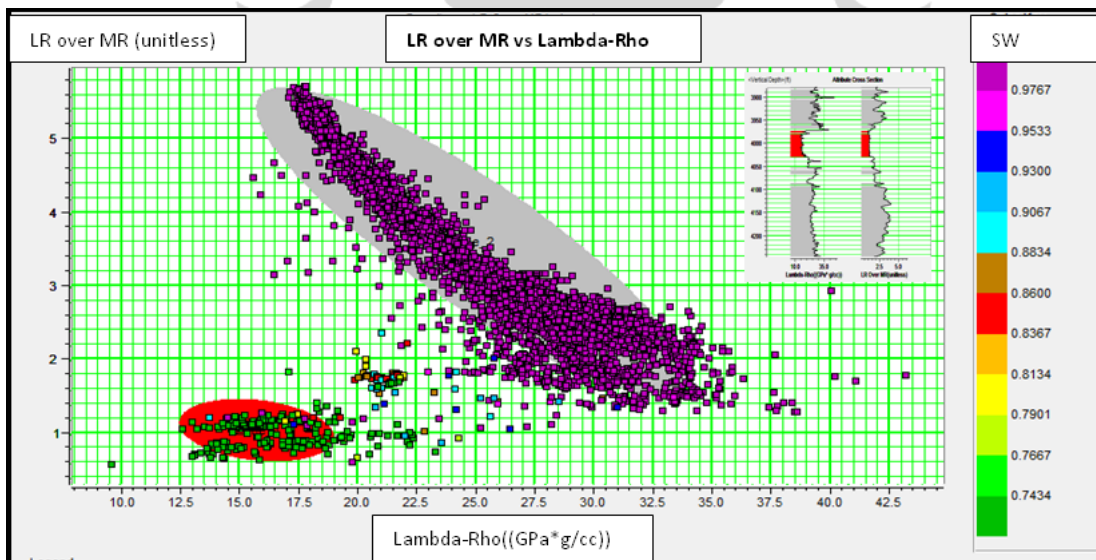

Figure 4.9 Cross plot Lambda-rho over Mu-rho and Lambda-rho with color from water saturation

Table 4.1 Rock physics analysis (Goodway's , 1997)

TABLE 1	Vp (m/s)	Vs (m/s)	ρ (g/cc)	Vp/Vs	(Vp/Vs)²	σ	λ + 2μ	μ	λ	λ/μ
Shale	2898	1290	2.425	2.25	5.1	0.38	20.37	4.035	12.3	3.1
Gas Sand	2857	1666	2.275	1.71	2.9	0.24	18.53	6.314	5.9	0.9
Avg. Change	1.40%	25%	6.40%	27%	55%	45%	9.20%	44%	70%	110%

(Moduli λ, μ are in GPa's)

Sensitivity analysis was performed using existing well logs data. The result showed that the well logs data were sensitive enough to discriminate between gas sand and shale at UG Massive formation. Therefore, it can be used for inversion process.

4.4 Well Seismic Tie and Wavelet Estimation

A well seismic tie requireS-wavelet estimation in order to generate a synthetic seismogram as a product of sonic and density. This is done by correlating the real seismic trace at the well location with a synthetic seismogram obtained from convolution of wavelet with reflection coefficients while the estimation of wavelet should be appropriate in order to produce the best match or correlation between synthetic seismogram and the real seismic trace. The goal of this correlation is to get the best match qualitatively and quantitatively with the highest correlation coefficient $(0-1)$. A high quality correlation between the seismic and synthetic trace is essential to create a valid inversion.

Beside common method to extract a wavelet such as Ricker or Band pass, a wavelet can be extracted from another two methods, statistical method and well method. A statistical method uses data such as a seismic volume, offset information and survey area with extraction window. The well method uses the same data as the statistical method, but also uses the well data. In this study the well method was used to extract the wavelet, because the wavelet from use well method has higher

coefficient correlation and also has the same zero phase as seismic data. The wavelet is extracted from three different 3D seismic volumes with 3 different angels, there are near, mid and far.

In this study wavelets were extracted from seismic data at an interval of 1000 – 1500 ms with a wave length 100 and taper length 20 to minimize the unwanted side lobes. Wavelet extractions were optimized to get the maximum correlation coefficient for each wavelet used in the correlation using the Javaz-4 well. The result was a good wavelet where well extracted wavelets are closer to zero phase, consistent with the seismic phase.
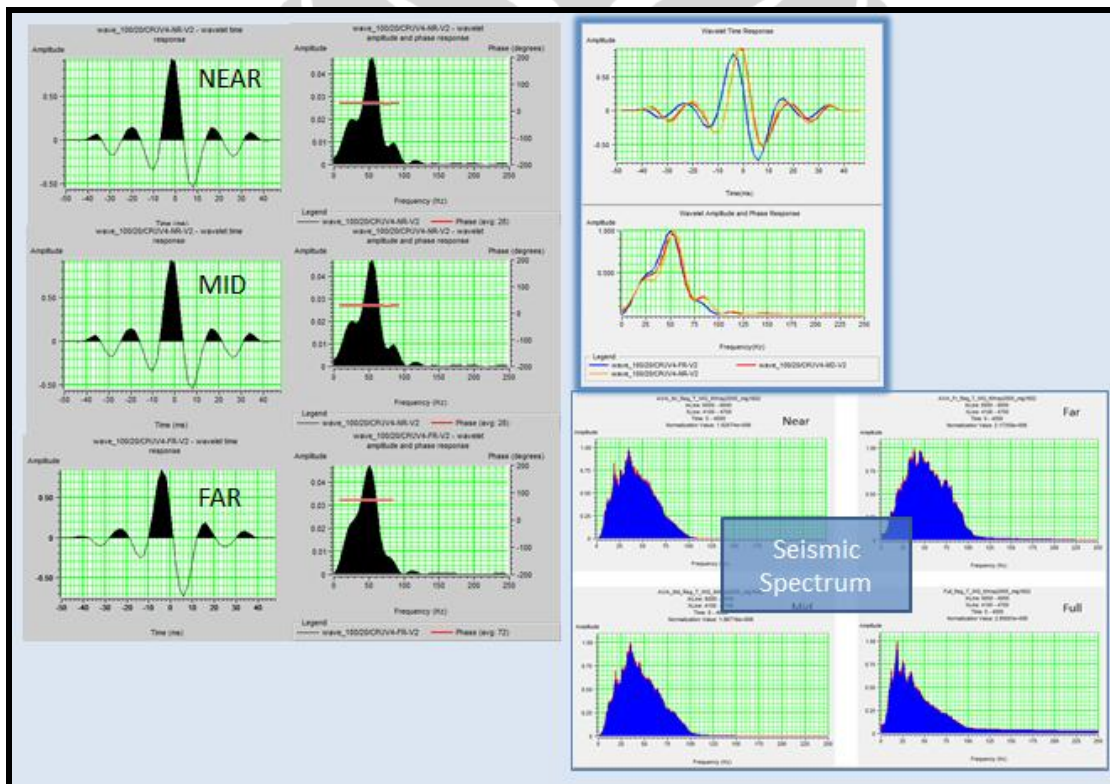

Figure 4.10 Wavelet estimation and seismic spectrum from seismic

The convolution process between wavelet and reflectivity series will form a seismogram synthetic. The seismogram synthetic will then be compared with the real seismic trace. The result from synthetic seismogram and correlation with seismic trace for near, mid and far in Javaz-4 well is shown as in Figure 4.11. Here we can

see that from this process we get the best maximum correlation value, 0.810 for near, 0.768 for mid and 0.665 for far with 3 ms time shift.
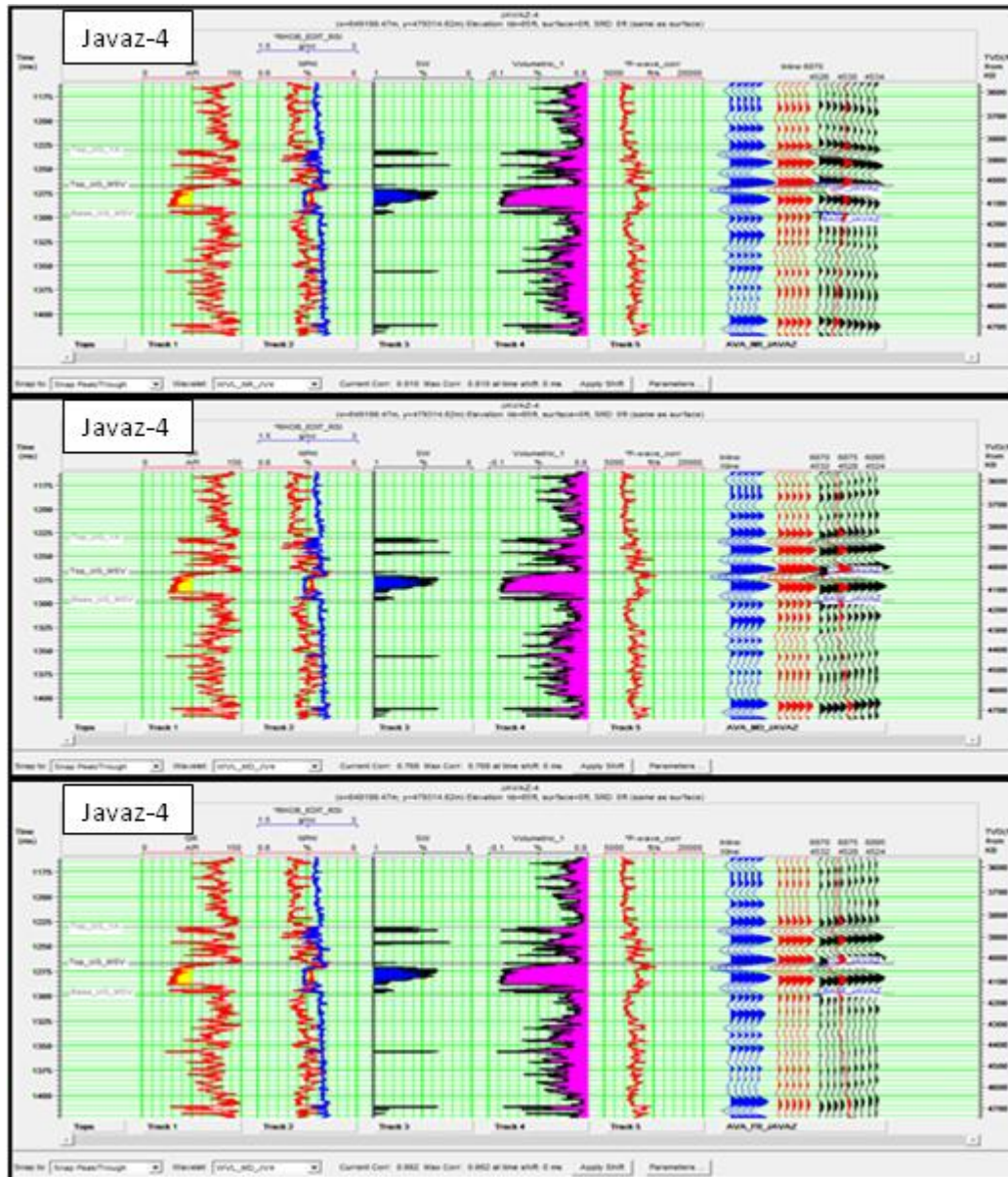

Figure 4.11 Correlation for near, mid and far at well Javaz-4

4.5 Horizon and Fault Interpretation

To interpret horizons and faults a full stack 3D seismic migrated volume was used. The first step in the process was interpreting the faults. Faults were picked every 10 x-lines and 50 inlines then correlated between fault segments. Next, reflection horizons which were related to geological well events were identified using the synthetic seismic tie. These horizons were picked on the same increment as the fault interpretation then interpolated. Horizons were initially picked on an arbitrary line between Javaz-4 and Javaz-1A as shown in Figure 4.12 and extended using an inline and x-line looping technique. In this study, there are 2 interpreted horizons: Top_Javaz and Base_Javaz. Figure 4.13 and 4.14 shows these 2 interpolated horizons.
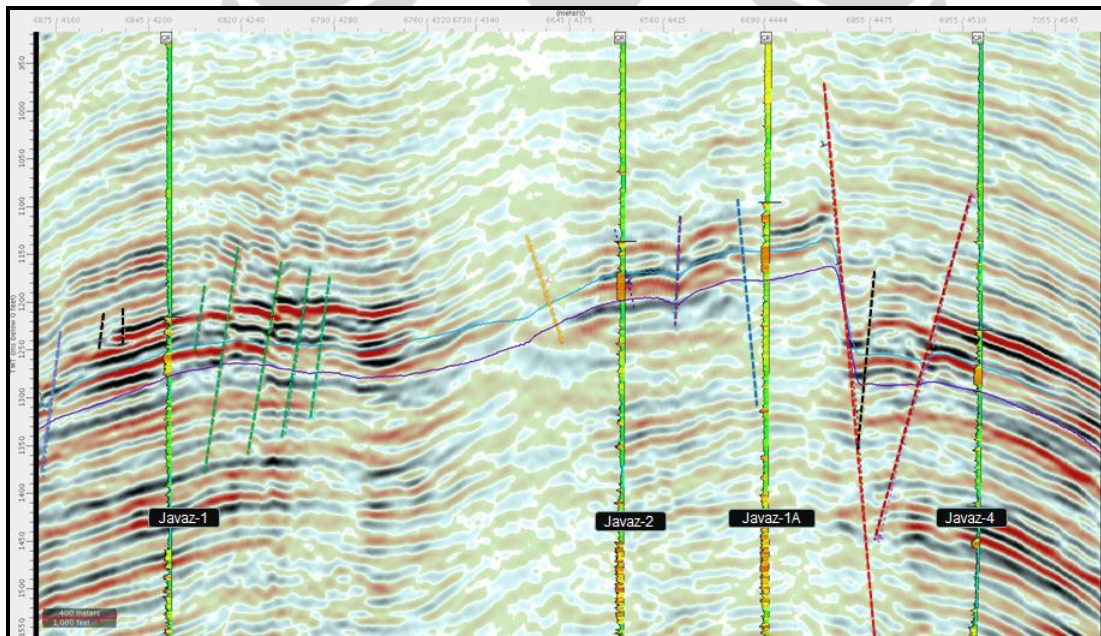

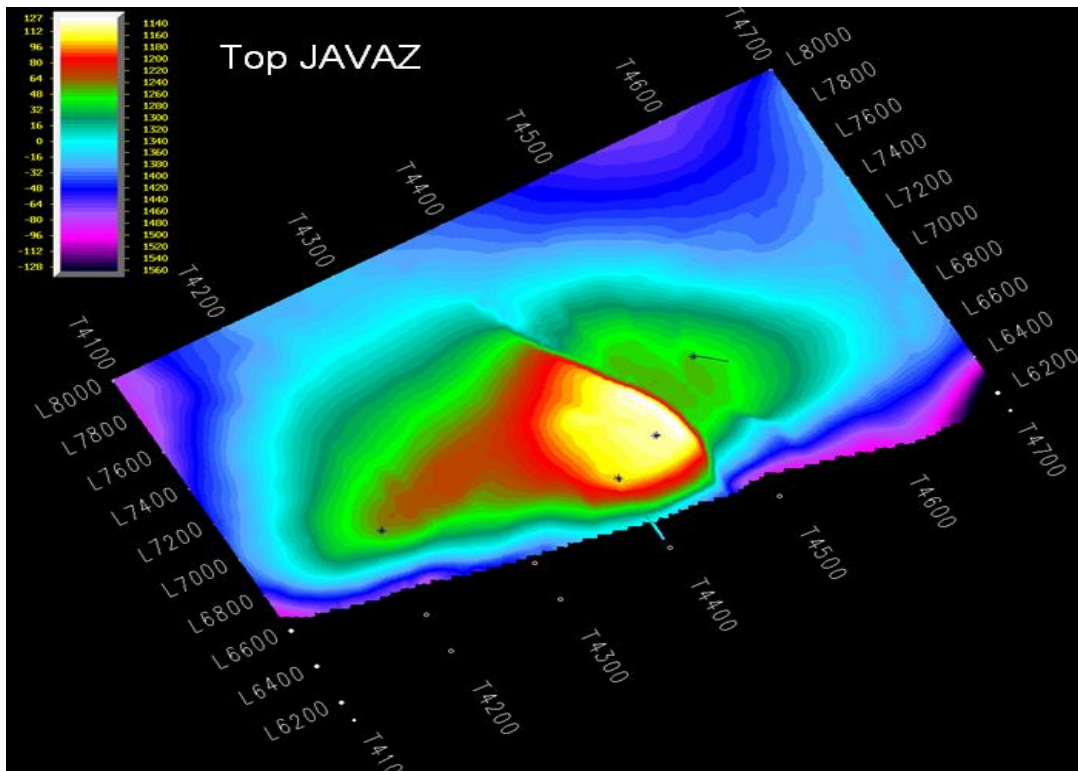Figure 4.12 Horizons and fault interpretation at Javaz-1A, Javaz-2, Javaz-3 and Javaz-4, arbitary line
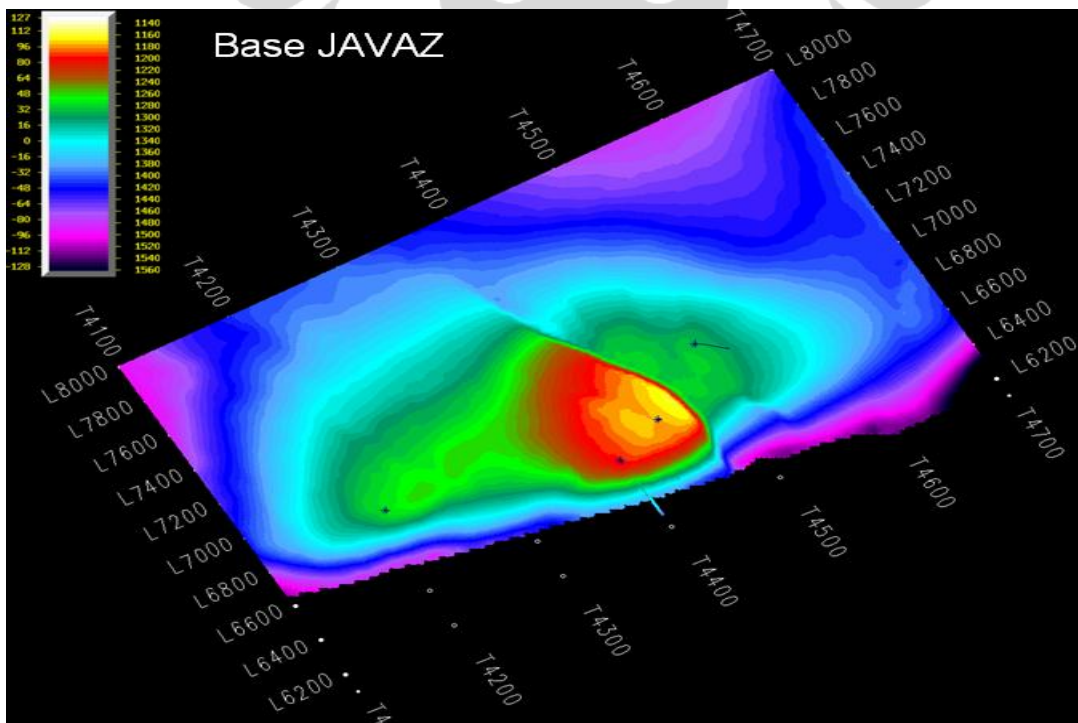
Figure 4.13 Top_Javaz Time Map

Figure 4.14 Base_Javaz Time Map

University of Indonesia

4.6. Low Frequency Model

Prior to the simultaneous seismic inversion process it is necessary to create a geological model. This geological model is known as a low frequency model or Initial model. To create this model, we need to have a well data set of P-wave velocity, S-wave velocity and density logs as references to create impedance volumes. Horizon interpretation data is then used to extrapolate P, S and density impedance values throughout the seismic volume. Using this process, low frequency missing from the seismic data needs to be recovered. This can be accomplished by applying a bandpass time domain filter to the interpolated model. For this case, the model was filtered to remove frequencies below 5 Hz and above 10 Hz. Figures 4.15, 4.l6, and 4.17 show examples of the P, S, and density impedance volumes after extrapolation and filtering.
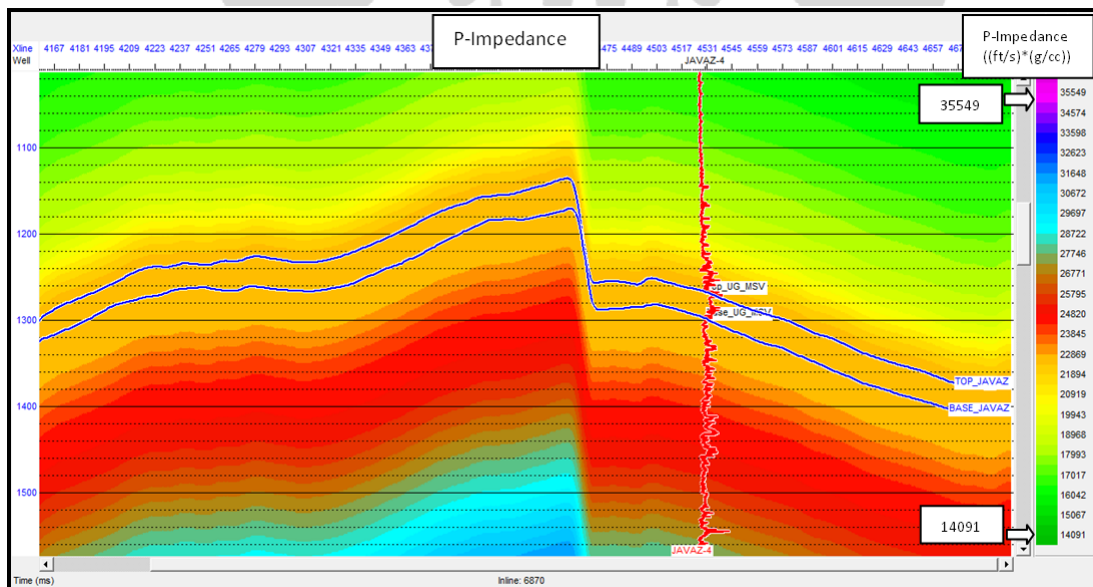

Figure 4.15 Initial model Zp section at Javaz-4 well location, inline 6870, x-line 4530
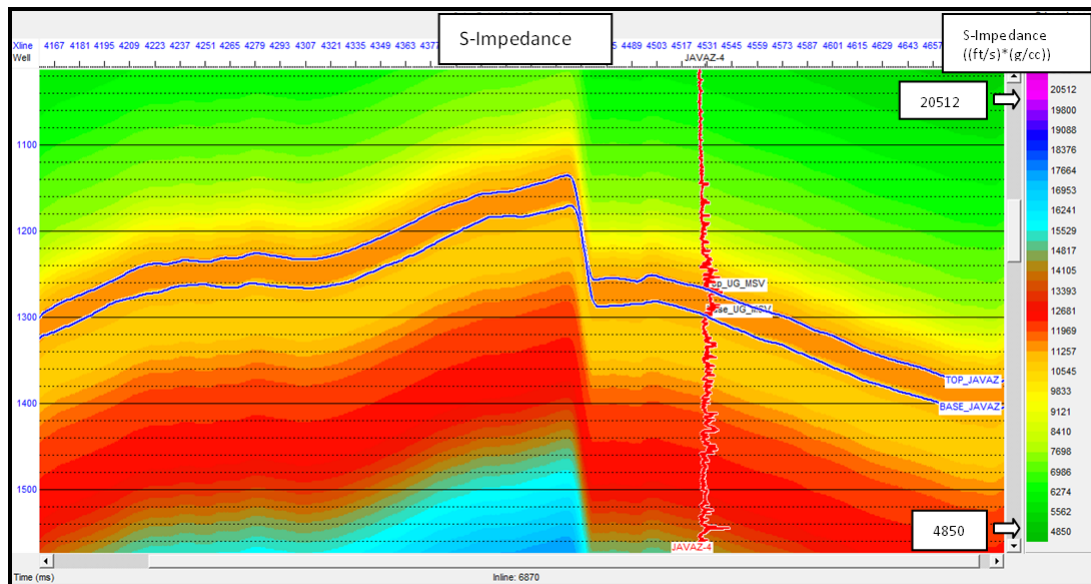
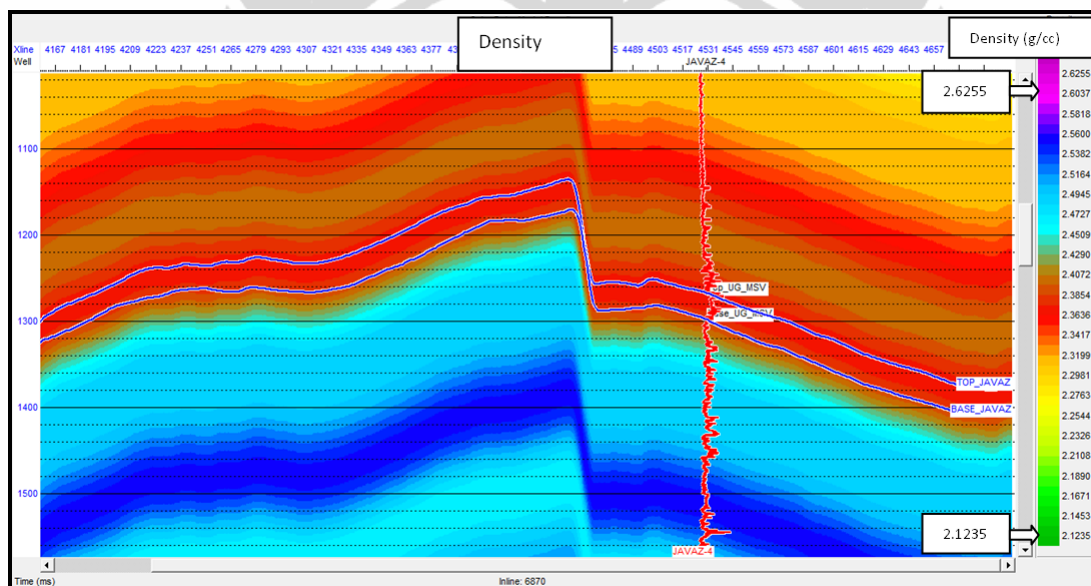Figure 4.16 Initial model Zs section at Javaz-4 well location, inline 6870, x-line 4530

Figure 4.17 Initial model Dn section at Javaz-4 well location, inline 6870, x-line 4530

4.7 Pre Inversion (QC) Analyses

Pre Inversion QC analysis consists of performing an inversion on selected well locations and testing a range of inversion parameters. The goal is to see how

well the analysis inversion succeeded or to compare different parameters before performing the actual simultaneous inversion. The inversion parameters are reflecting the background relationship between ln(ZP), ln(ZS), and ln(Density) which written on equation on Chapter 3. They are extracted from the regression linear trends drawn on cross plot ln(ZP) versus ln(ZS) and ln(ZP) versus ln(Density) as the regression coefficient – k, kC, m, mC, ΔLS, ΔLD (Figure 4.18). These coefficients are then displayed in the inversion QC analysis window to determine the quality of the correlation. Figure 4.19 is an example which shows a good correlation coefficient 0.985.
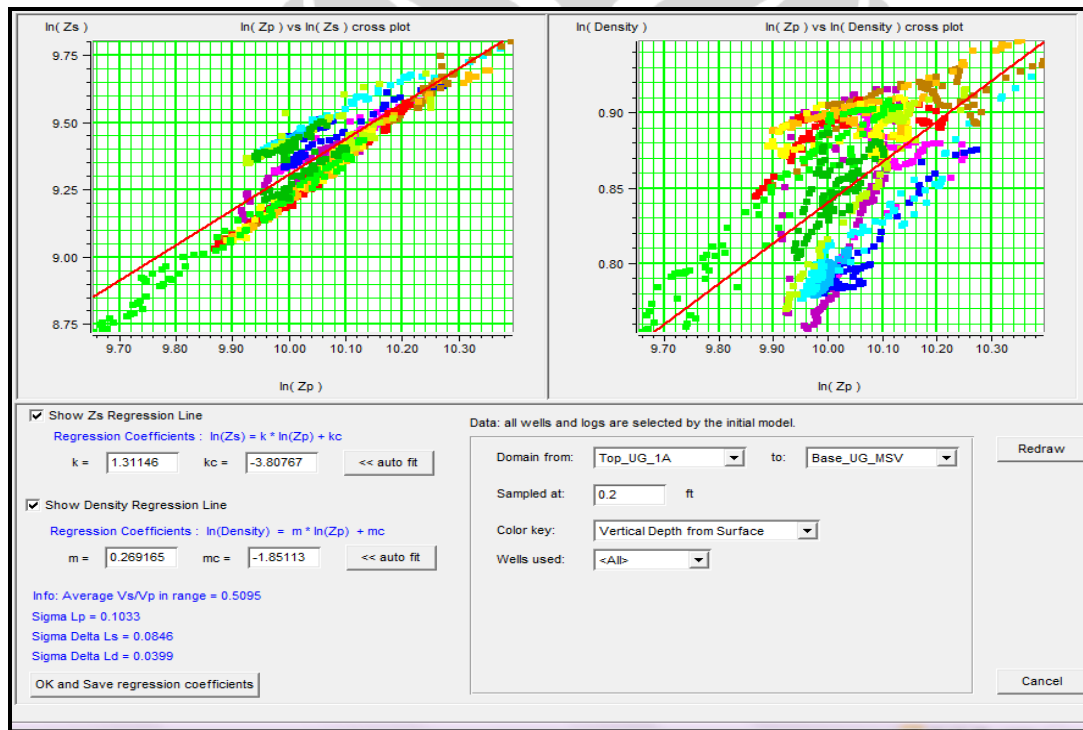

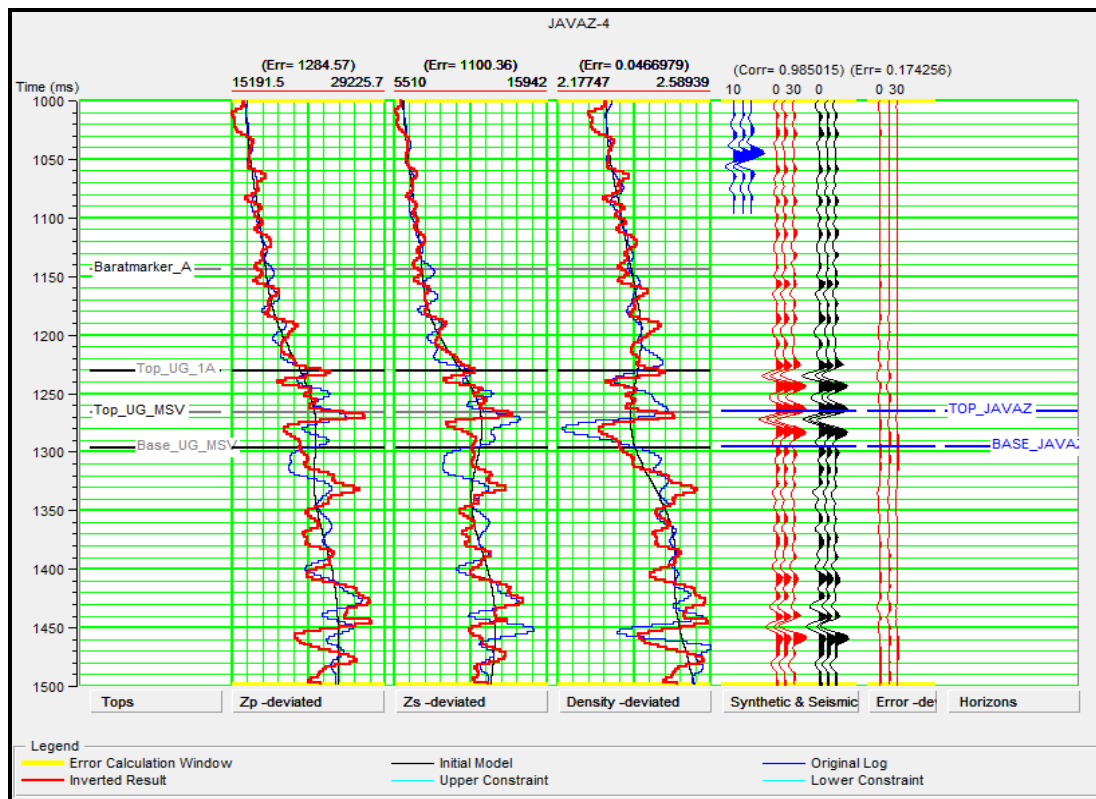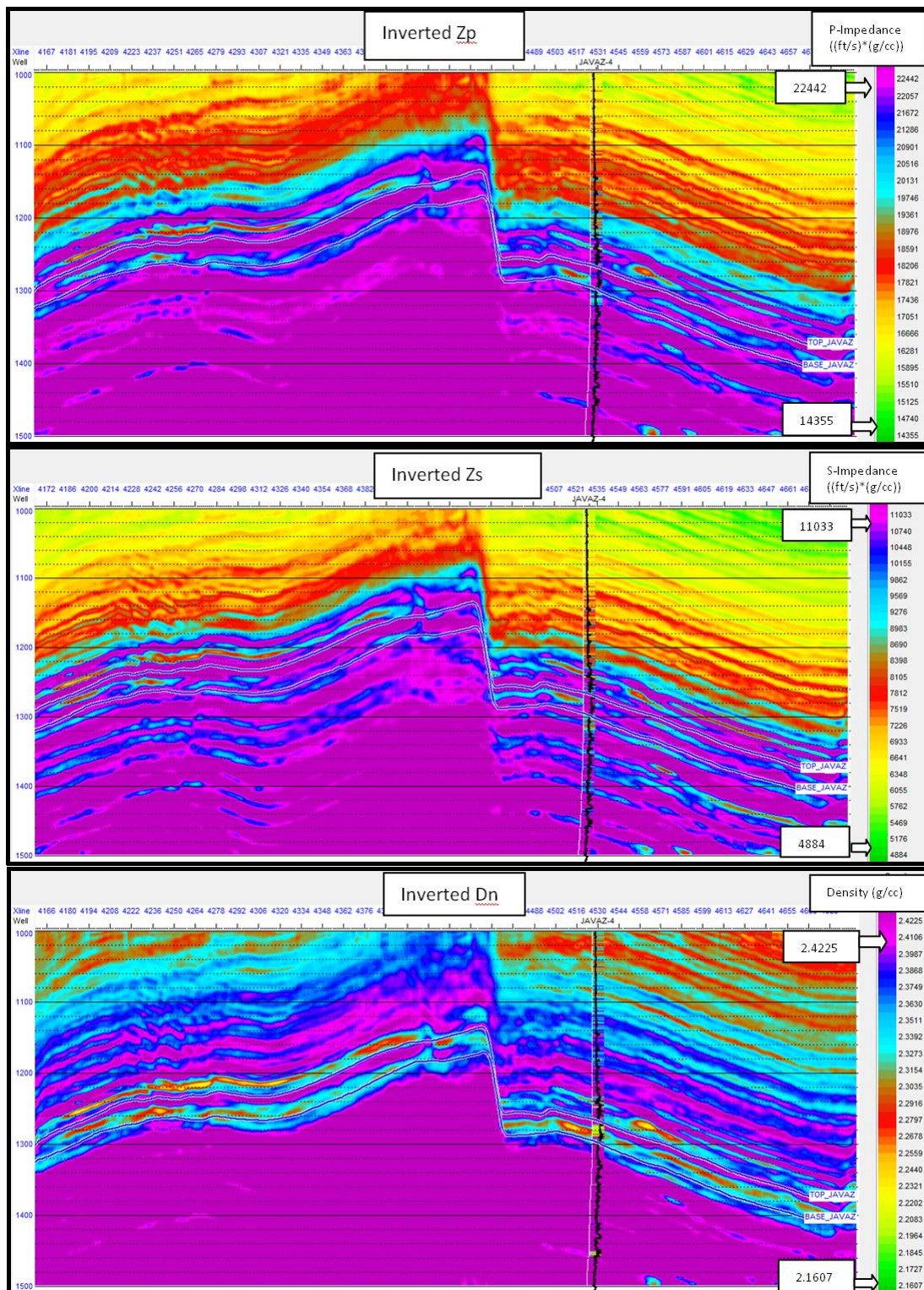Figure 4.18 Linear trend regression line between ln(Zp), ln(Zs), ln(Dn) and the coefficient regression

Figure 4.19 Inversion analyses at well Javaz-4 showing good correlation between seismic inversion and log curve

4.8 Simultaneous Inversion

The simultaneous inversion process applied in this study uses Fatti's version of the Aki-Richard's equation which models reflection amplitude as a function of incident angle, using initial model P-impedance (Zp) volume, S-impedance (Zs) volume, Densisty (ρ) volume, as well as the angel of incidence and Vp/Vs as the input. The result from Fatti's equation is then used to create synthetic seismic traces by convolving with an angle dependent wavelet (near, mid and far). This process is continually repeated until it achieves the smallest least-squared error between the synthetic seismic trace and real seismic trace. In this study the interval target for this simultaneous inversion process is constrained between 1000 ms to 1500 ms due to lack of time and disk space. The result at the well section of Javaz-4 and Javaz-3 are showed at Figure 4.20 and Figure 4.21

Figure 4.20 Inversion result at Javaz-4, first panel is inverted Zp, second panel is inverted Zs and third panel is inverted Dn

University of Indonesia

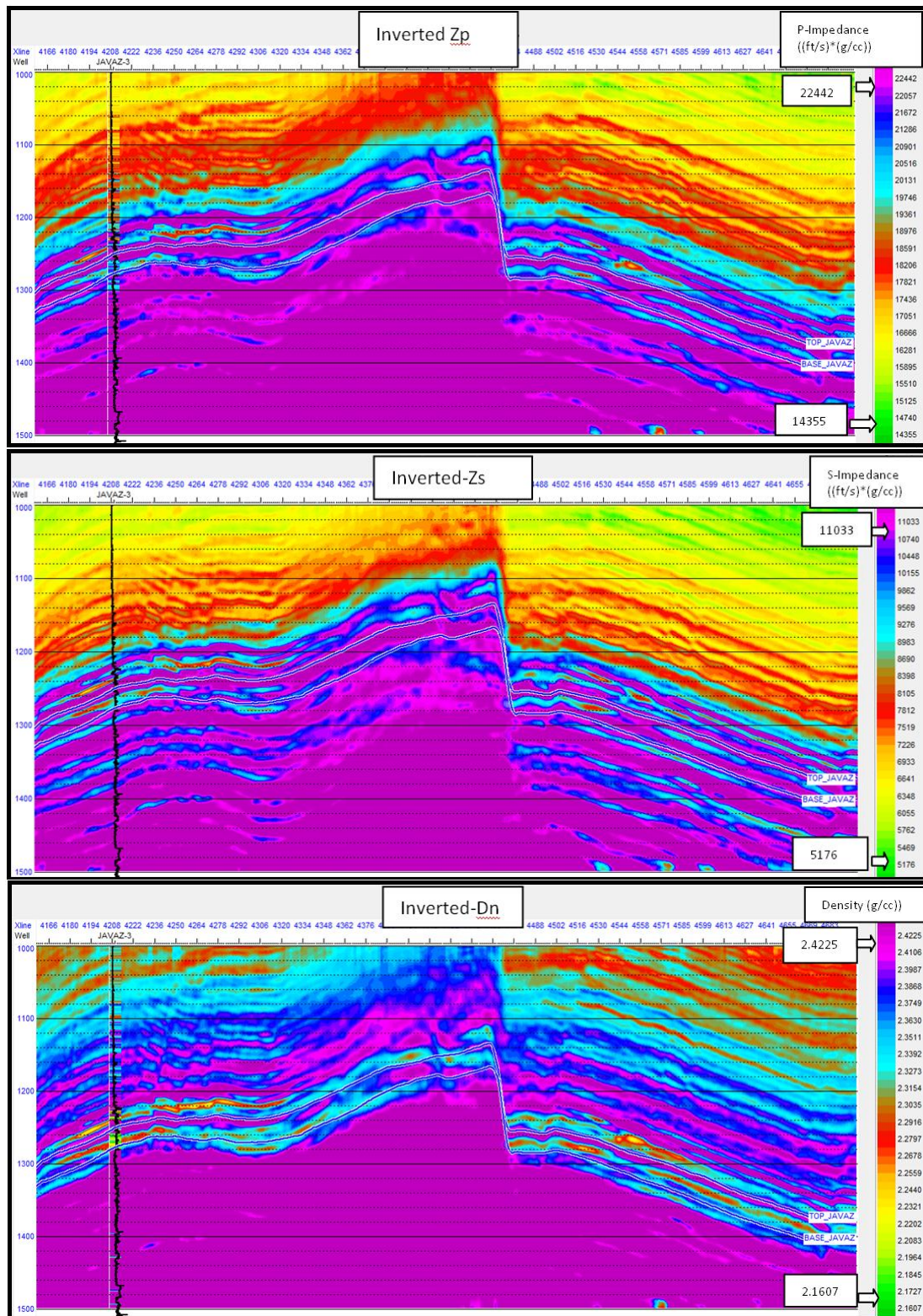Figure 4.21 Inversion result at Javaz-3, first panel is inverted Zp, second panel is inverted Zs and third panel is inverted Dn

4.9 Lame Parameter Transformation

After inverting the near, mid and far volumes to become inverted P-impedance (Zp), inverted S-impedance (Zs) and inverted density (Dn), these results can then be transformed into the Lame parameters which are Lambda-rho, Mu-rho and lambda-rho over mu-rho. This transformation results from the relational equations between velocity P-wave (Vp), velocity S-wave (Vs) and Lame parameters. Based on the algorithms presented in Chapter Three, equations (3.4) and (3.5) can be converted to become equation (3.11) and (3.12) and from these equations we will arrive at equation (3.13)

Based on the equation above, parameters for Lambda-rho, Mu-rho and lambda over mu can be derived from the inversion results P-wave impedance and S-wave impedance. Hampson Russell software's Trough Trace Math was conducted on every trace from each seismic volume from inversion result to determine the correct parameters, calculated as:

$$\mu\rho = (\text{S-wave volume impedance} - \text{S})^2 \qquad\qquad (4.1)$$

$$\lambda\mu = (\text{P-wave volume impedance} - \text{P})^2 - 2 \times \mu\rho \qquad\qquad (4.2)$$

Figure 4.22 and 4.23 show the results from the process of P-wave volume impedance (Zp) and S-wave volume impedance (Zs) to become Lambda-rho, Mu-rho and lambda-rho over mu-rho using simultaneous inversion method.
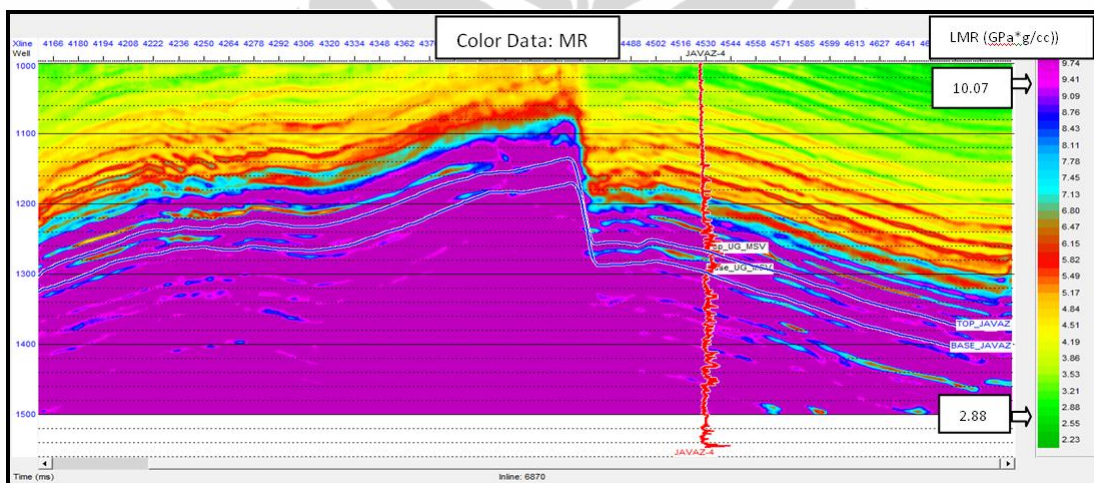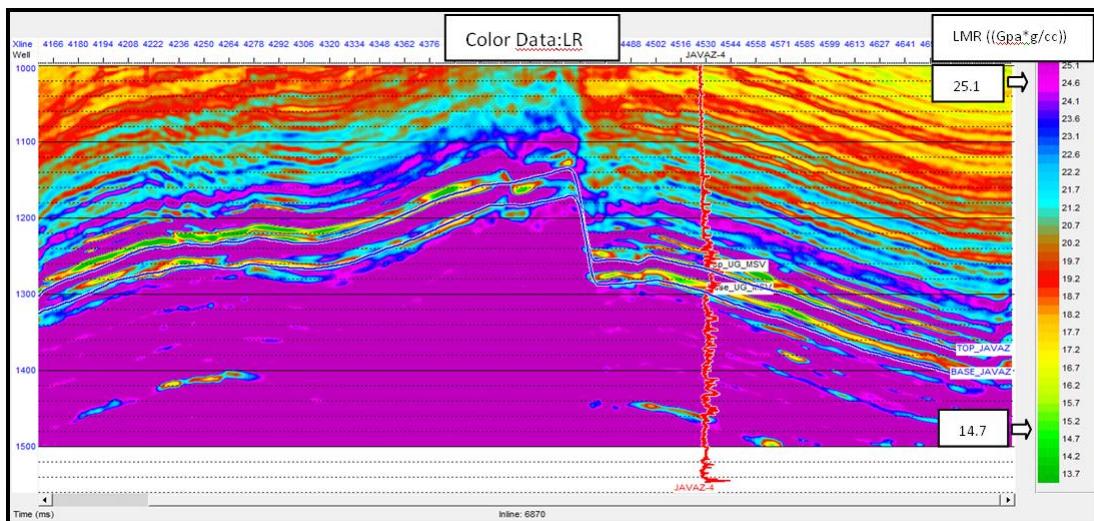
Figure 4.22 Lambda-rho and Mu-rho volumes derivative of Zp and ZS-impedance volume at well Javaz-4
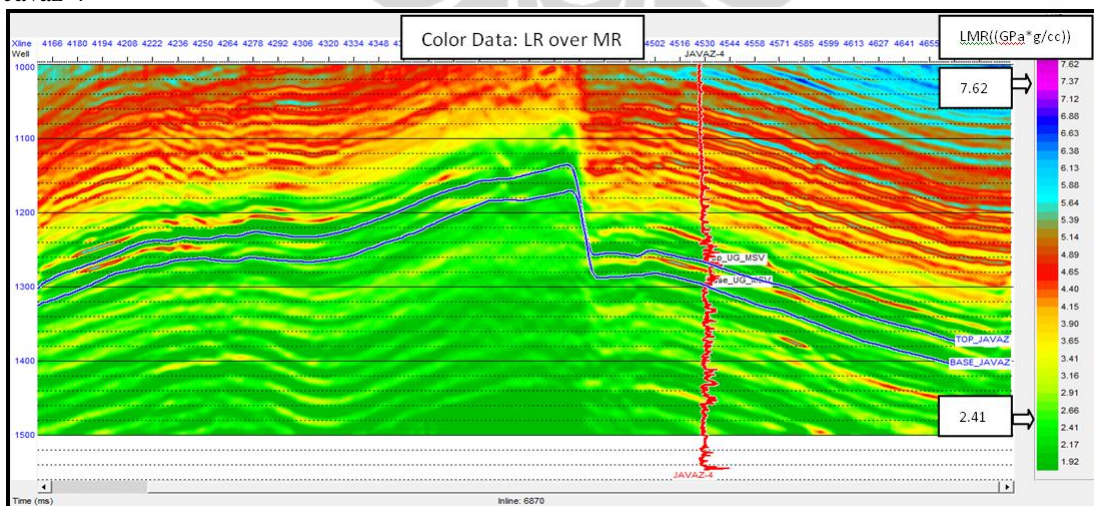

Figure 4.23 Lambda-rho over mu-rho volume at well Javaz-4

CHAPTER 5

RESULT AND DISCUSSION

The results of the simultaneous inversion described in Chapter 4 (P-impedance, S-impedance and density volumes) can be further analyzed and interpreted.

5.1 Rock Physics Template

Rock physics templates were produced by crossplotting the various attributes calculated from well logs in the UG Massive reservoir. The crossplot relationships can then be used as a reference in mapping rock physics properties to the seismic data. Crossplotting Lambda-rho over Mu-rho vs. Lambda-rho (density) from the Javaz-4 well helps distinguish between the effects of rock and fluid in the zone of interest. Figure 5.1 shows the cross plot volume Lambda-rho over Mu-rho and Lambda-rho which are extracted from the inversion results at the well location into the rock template.
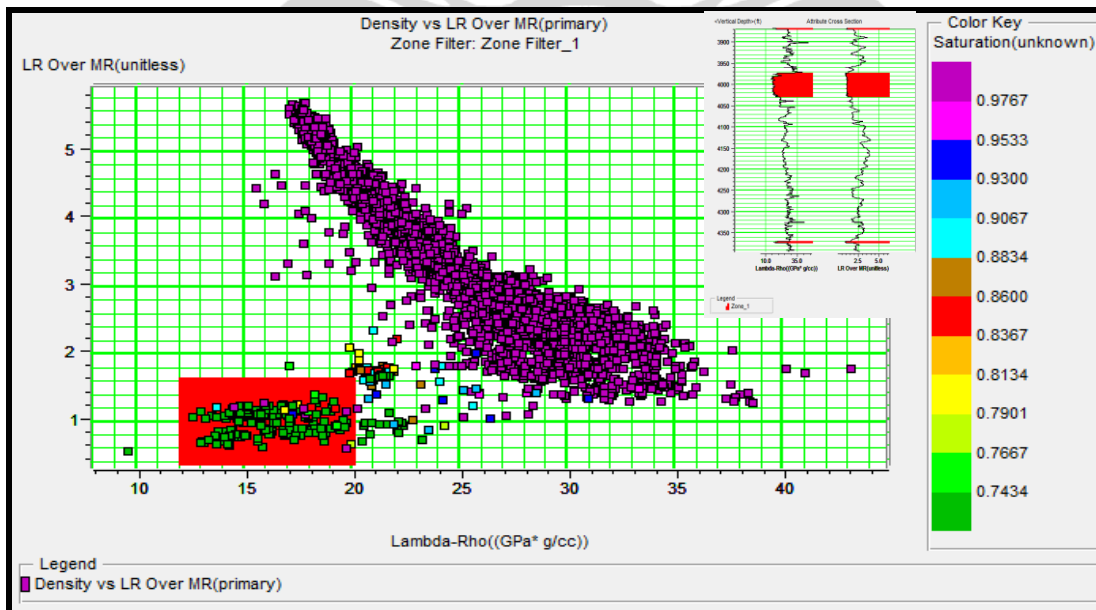

Figure 5.1 Cross plot between Lambda-rho and Lambda-rho over Mu-rho from well

A crossplot is used to test whether the inversion results can be used to distinguish or classify rocks and fluids, as well as to examine whether the grouping remains consistent with the crossplot from the well data. Figure 5.2 show that the volume inversion result is extracted in the reservoir interval shows good grouping for lithology and fluid. Also the well values crossplot in the expected zone where both lambda-rho over mu-rho and Lambda-rho are in the minimum range in the gas bearing zone. The fit is not perfect, but is still within the expected position, and also has a consistent trend. This is quite reasonable due to differences in sample interval and vertical resolution between the datasets..
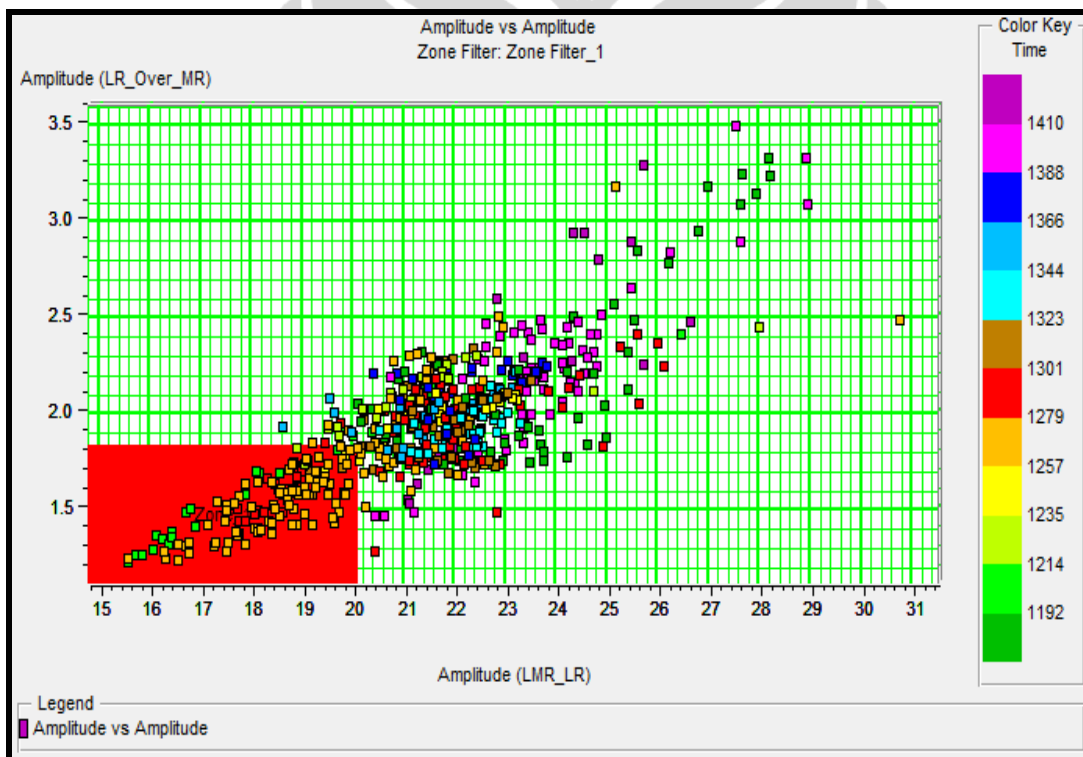

Figure 5.2 Crossplot results of Lambda-rho over Mu-rho and Lambda-rho extracted from inversion result at the interval zone.

So based on the above results of well data and inverted seismic volume cross plot, it can be seen that a difference can be established in the volumes between shale and sand zones. This result can be seen more clearly in crossplot volume.

5.2 Cross Plot Volume

After establishing the pattern between the well and crossplot volumes, the next step is to bring the crossplot of non-hydrocarbon gas bearing and hydrocarbon bearing to the seismic cross sections volume with different in colors, as shown in Figure 5.3 below, is a cross plot on Javaz-4 well locations shown on the seismic section
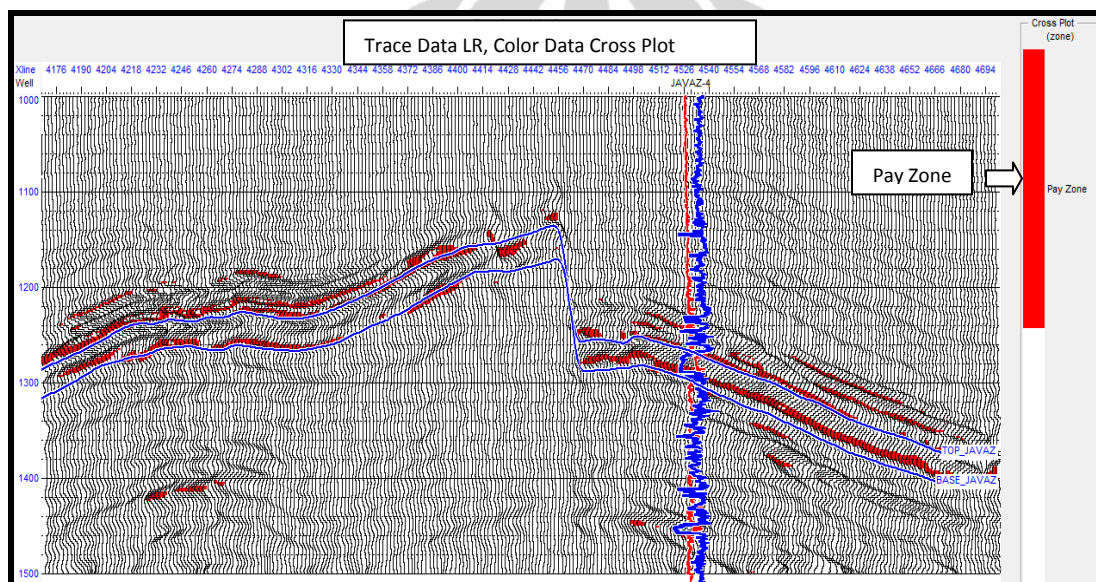

Figure 5.3 Cross plot volume section at well Javaz-4, Red color is showing gas zone

From the cross plot volume section above we can see that the Red color between top and base from the rock physic template is showing gas zone distribution at Javaz-4 well in UG Massive reservoir. The grey or red color outside the top and base can be said as the zone area of non-hydrocarbon or another formation outside UG Massive, and it could be shale, wet sand or shaly sand.

5.21. Blind Test

The blind test is used to determine if the rock physics template from Javaz-4 can be applied to another well in this study such as Java-3, Javaz-2 and Javaz-1A, where these three wells were not involved in previous simultaneous inversion process. As can be seen in Figure 5.4, Javaz-3 is a good fit and could be used to predict hydrocarbon content, meanwhile Javaz-2 and Javaz-1A as shown in Figure 5.5 and Figure 5.6 do not fit the expected values. These wells are located in an area where the zone is not colored red.
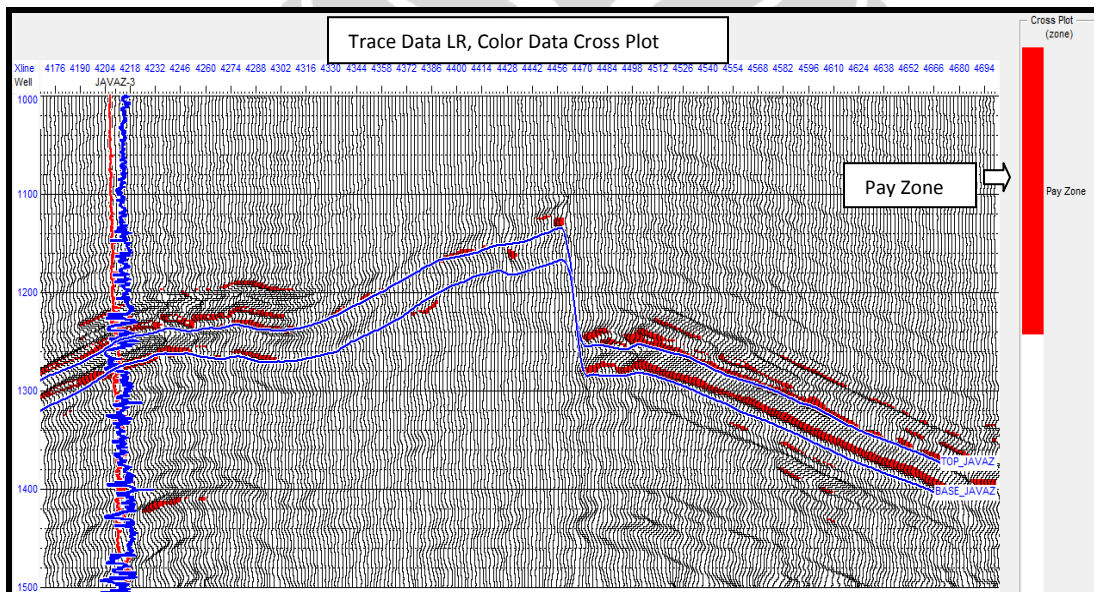

Figure 5.4 Blind test from rock physics template at Javaz-3, Red color is showing gas zone

Figure 5.5 Blind test from rock physics template at Javaz-2, target reservoir Red color is not showing gas zone
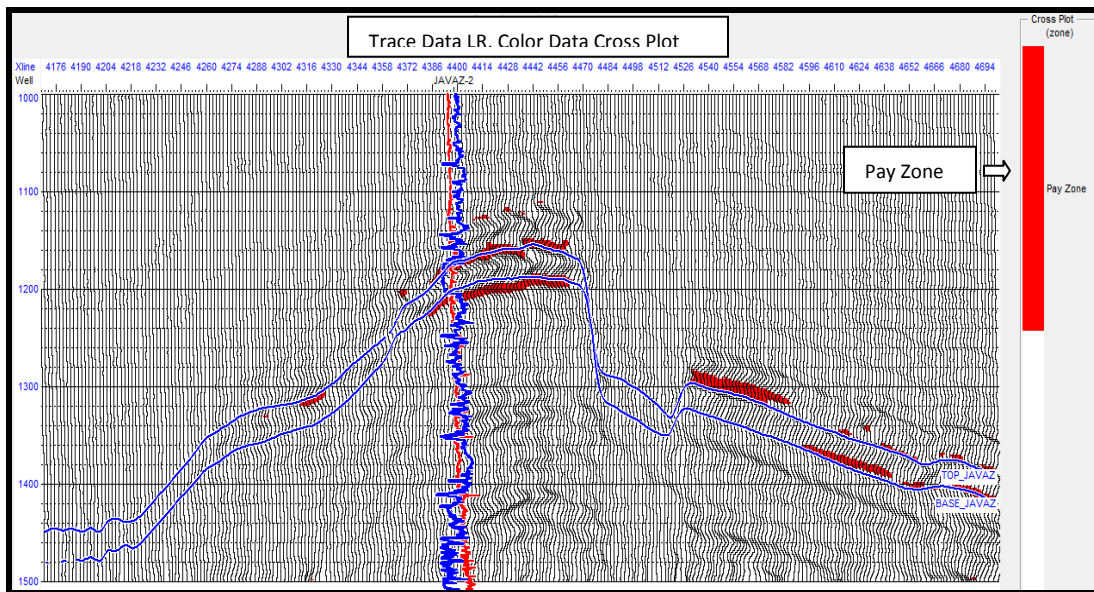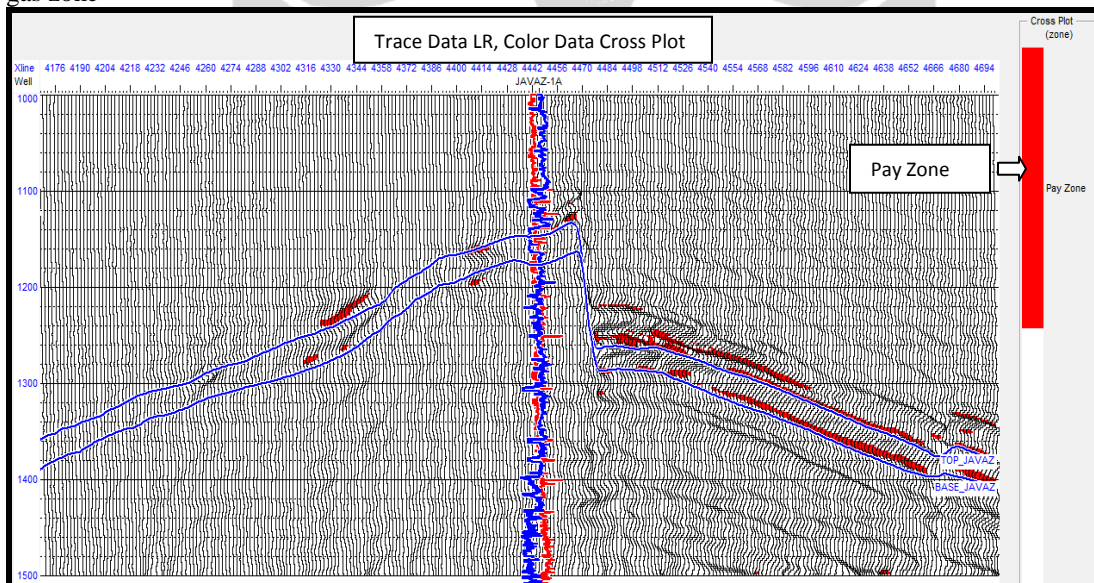

Figure 5.6 Blind test from rock physics template at Javaz-1A, target reservoir Red color is not showing gas zone

5.22. Horizon slicing

Horizon slicing can be used to look at the distribution of gas bearing and non-hydrocarbon bearing zones in a lateral or horizontal perspective, by using volume extraction along the reservoir zone, as shown at Figure 5.7. This horizon slice is

extracted from the cross plot volume and rock physics template discussed before. It can be seen that the Javaz-3 well is still in the red zone where the distribution is quite wide. The Javaz-2 and Javaz-1A well lie in narrow red zone, separate from where Javaz-3 is situated.
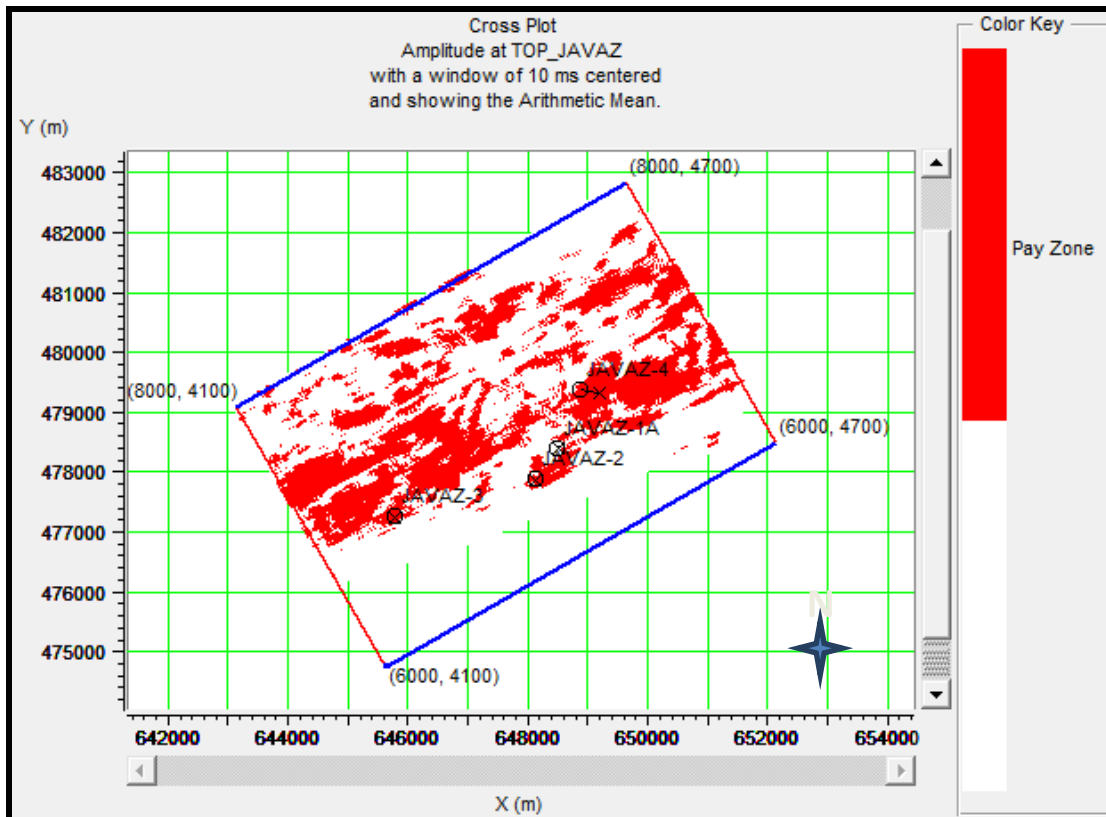
Figure 5.7 Showing horizon slice a long base Base_Javaz horizon at Javaz reservoir which reflect gas accumulation.

5.3 Pore Gas Prediction

Pore gas can be predicted using a Lambda-rho volume that is created from P-impedance and S-impedance volumes using equation (3.13) as discussed in Chapter 3. Lambda-rho or incompressibility is a physical change in the pore space when subjected to pressure. This change is more often caused due to a change from the rock pores and fluid compared to changes of grain size. The easier media is pressed, equal to smaller value of incompressibility. Incompressibility is low in gas saturated

sandstone; therefore Lambda-rho can be used as gas content indicator in the pore space. Figure 5.8 shows the area where the dotted white line shows the distribution low value of Lambda-rho, which is associated with the pore gas area equivalent to sand stone reservoir.
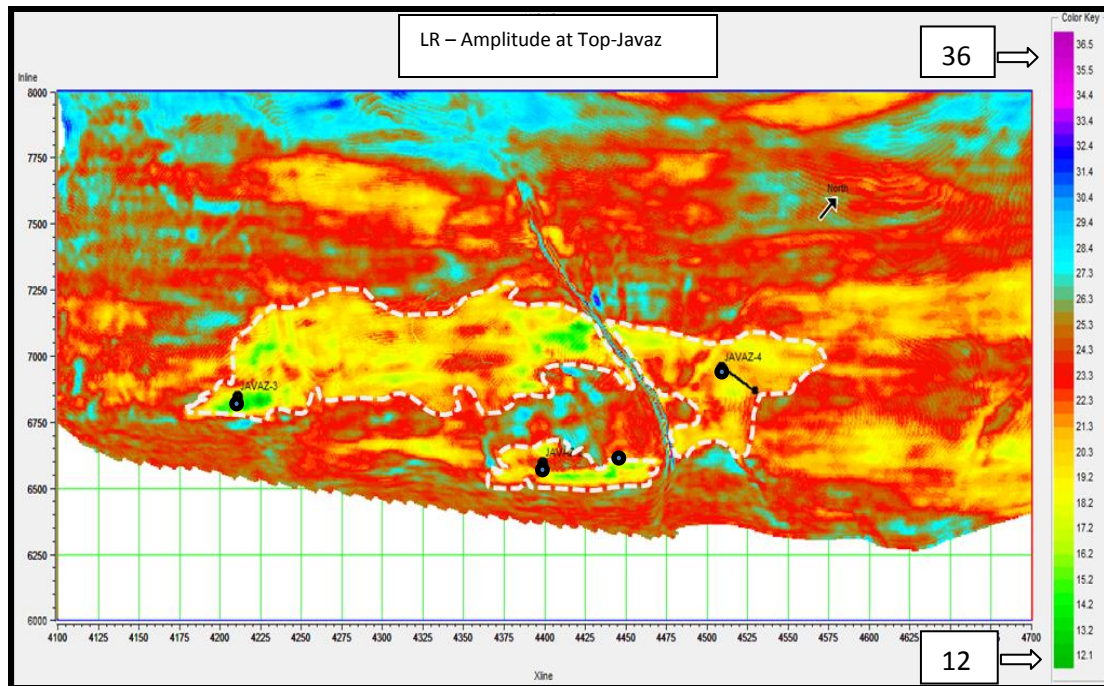
Figure 5.8 The dash lines are area where the incompressibility value is low

Based on the interpretation and analysis above, it can be concluded that the sandstone with good quality and accumulation of gas from the reservoir UG Massive is separated into several compartments which could be a result of the fault structure and compartmentalization in this field. The Lambda-rho volume slice along the horizon can be used to identify areas that are prospective for exploitation, as shown in Figure 5.8 above.

5.4 Porosity Prediction

Porosity prediction is accomplished using the porosity volume created from the P-impedance volume. A crossplot of NPHI (Neutron Porosity) with P-impedance from the Javaz-4 well data shows a trend separation between the zone containing hydrocarbon and non-hydrocarbon as shown in the Figure 5.9. The color key is tied to the water saturation data from the Javaz-4 well. By using a regression line through pay trend will get the following equation:

$$y = -1.72518 * 10 - 5x + 0.6303107$$

Where y = Porosity

  x = P-impedance

This equation can be used to get porosity volume with input from P-impedance inversion volume.

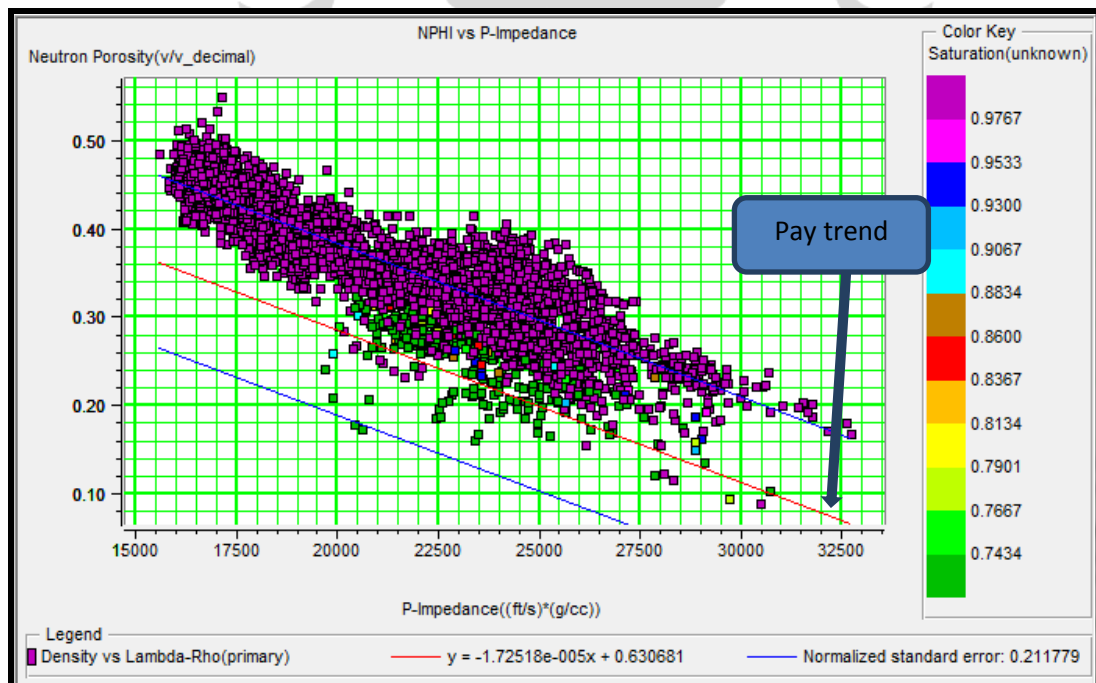Figure 5.9 Showing trend hydrocarbon zone (pay) and non-hydrocarbon (wet)

The equation can be used with the amplitude volume and an extraction along the Base UG Massive in Javaz field to create a porosity attribute map as seen in Figure 5.10.   Blue to purple values indicate good porosity areas.
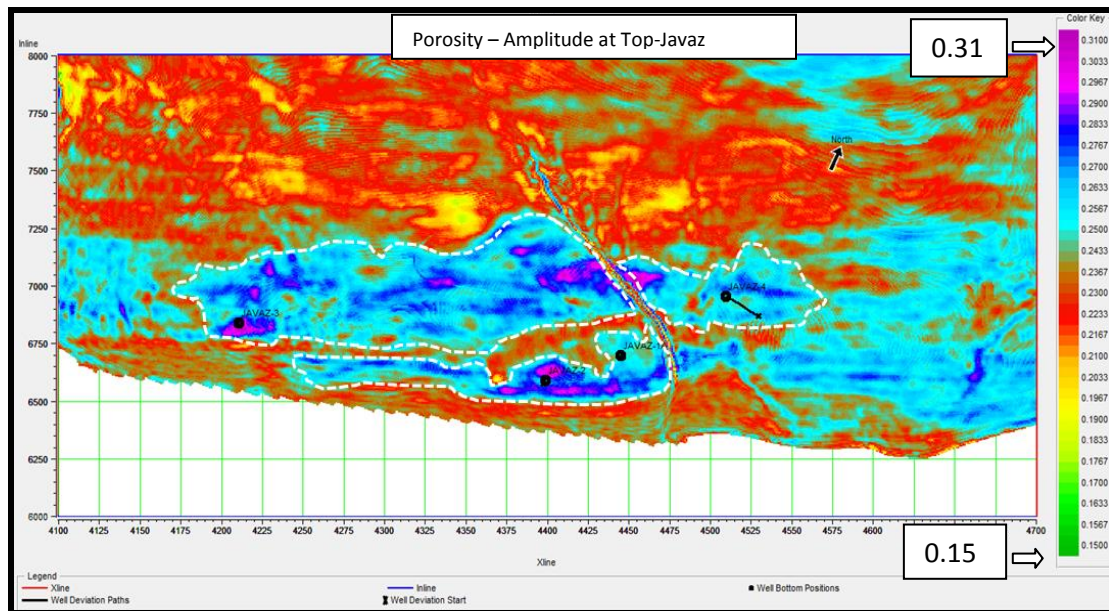

Figure 5.10 Shows porosity map where porosity ranging from 20% up to 30% is observed as reservoir

CHAPTER 6
CONCLUSION AND RECOMENDATION

The study contained in this thesis shows that the Seismic Simultaneous Inversion Method can be successfully used to discriminate between sand and shale in clastic reservoir zones and that it can also be used to define hydrocarbon bearing and highly porous areas.

6.1 Conclusion

1. Through seismic simultaneous inversion method from feasibility study to inverted volume (Zp, Zs and Dn) and also using derivative volumes (Lambda-rho, Mu-rho and Lambda over Mu), it can be concluded that there is a relationship between rock physics (Zp, Zs, Vp/Vs) and rock properties (density, porosity, gas saturation, shale volume) in the Javaz field.

2. Hypothesis is proven that seismic simultaneous inversion can be applied in this study area and can be used to estimate P-impedance, S-impedance and Density volume where these volumes are representing Java's reservoir. Through Pre-inversion QC analysis a good correlation and similar trend can be established between inverted log results and the original log at the well location. This has also been shown to be applicable in blind test well locations where the reservoir characterization is consistent with the actual well location.

3. The seismic simultaneous inversion and the derivatives volumes can be combined with the rock physics character where we can have a good result as quantitative and qualitative, such as porosity and gas distribution, geometry and connectivity trough cross plot volume section and slice map at horizon target. Porosity is ranging approx. at 25% up to 30% and Lambda-rho is ranging from 13 (GPa*g/cc) up to 25 (GPa*g/cc) with reservoir characterization value approx. at 13 (GPa*g/cc) up to 18 (GPa*g/cc) or can be concluded as low incompressibility values are associated with gas sands,

meanwhile value range for Mu-rho is ranging from 2 (GPa*g/cc) up to 10 (GPa*g/cc) with reservoir characterization value approx. at 6 (GPa*g/cc) up to 10 (GPa*g/cc) or can be concluded as high rigidity values are associated with sands.

4. The seismic simultaneous inversion method can be used to predict gas distribution in the UG Massive reservoir in Javaz field. From Javaz-4 and blind test well at Javaz-3, but not for Javaz-2 and Javaz-1A. Base on this result this seismic simultaneous inversion method can be used as a tool to predict reservoir hydrocarbon characterization.

5. Using crossplot analysis and horizon slices of pore gas or porosity combined with a structure map, it can be concluded that in within the UG Massive formation at Javaz field there are some more potential areas where gas accumulations exist. These areas show potential for further studies or exploration activities. Through analysis geometry distribution of pore gas and porosity it can be concluded that gas only exists on the highest value of porosity in UG Massive formation.

6.2 Recommendation

Through the application of seismic simultaneous inversion and recognizing the weakness of this process, this study is intended to become an alternative interpretation of mapped porosity and gas distribution. The technique applied in this study is not the only way to predict reservoir hydrocarbon characterization in Javas field. It is meant to generate a preliminary identification result and to develop a higher degree of certainty. The results of this study should be compared to the results from other methods to determine better comprehensive conclusions. Other suggested studies would include fault seal analysis to determine if the fault in the field is sealing and water saturation distribution or shale volume distribution analysis.

REFERENCES

Aki A., and Richard P.G., 1980, Quantitative Seismology: Theory and Methods, W.H. Freeman & Company.

Avseth, Per., Mukerji Tapan., Mavko, Gary., Quantitative SeismikInterpretation, Applying Rock Physics Tools to Reduce Interpretation Risk, Cambridge University Press.

Batzle, M. and Wang, Z., 1992, Seismic Proprties of Pore Fluids, Geophysics : Vol 57, no 11 (November 1992); P. 1396-1408

Castagna, J.P., Swan, H.W., and Foster, D.J., 1998, Framework for AVO Gradient and Intercept Interpretation, Geophysics, 63, 948-956.

ConocoPhillips Indonesia Internal Reports, Unpublished

Hilterman, F.J., 2001, Seismik Amplitude Interpretation, 2001 Distinguished Instructor Short Course, Series, No.4, Sponsored by SEG & EAGE.

Russell, Hampson, AVO Workshop Part 1 & 2, A CGG Veritas Company, CGG Veritas.

Rutherford, S., and Williams, R., 1989, Amplitude Versus Offset Variation in Gas Sand, Geophysics 54, 680-688.

Shuey, R.T., 1985, A Simplification of the Zoeppritz Equations, Geophysics 50, 609 -614.

Sukmono, S., 2002 An Introduction to Seismik Reservoar Analysis, in Seismic Inversion and AVO Analysis for Reservoar Characterization, Department of Geophysical Engineering ITB, Bandung

Suprajitno, M., 2000, Physical Aspect of Exploration Seismology, Geophysics Program of Mathematics and Sciences Department UI, Depok

Zoeppritz, R., 1919. On The Reflection and Propagation of Seismik Waves, Erdbebenwellen VIIIB; Gottinger Nachrichten I, 66-68.